IEEE Access
Multidisciplinary : Rapid Review : Open Access Journal

Received May 30, 2019, accepted June 11, 2019, date of publication June 21, 2019, date of current version July 30, 2019.

Digital Object Identifier 10.1109/ACCESS.2019.2924293

Review Paper on Transmitarray Antennas

JOAO R. REIS, MARIO VALA, AND RAFAEL F. S. CALDEIRINHA, (Senior Member, IEEE)
Instituto de Telecomunicações, 2411-901 Leiria, Portugal
Polytechnic Institute of Leiria, 2411-901 Leiria, Portugal

Corresponding author: Joao R. Reis (jvreis@co.it.pt)

This work was supported in part by the European Regional Development Fund (FEDER), PO CENTRO/SI-IDT, through the Project RADAVANT (03/SI/2017) under Grant 033907, through the Programme COMPETE 2020 of the Portugal 2020 framework, Project RETIOT, POCI-01-0145-FEDER-016432 and, in part by the Portuguese Government through the Foundation for Science and Technology (FCT) under Grant UID/EEA/50008/2019.

ABSTRACT This paper presents a thorough review of transmitarray devices particularly aiming antenna beamsteering, gathering some of the most relevant solutions published by the scientific community in the field. First, the background for realizing 1-D and 2-D antenna beamsteering with a transmitarray is introduced. Subsequently, several examples of unit-cells for transmitarray implementation and complete transmitarray designs presented in the literature are outlined. Each solution is analyzed in detail, identifying the nature of its layout, e.g., based on microstrip patches, frequency selective surfaces (FSS), or metamaterials (MMs), and the method employed to enable electronic reconfigurability, e.g., p-i-n diodes, varactor diodes, or microelectromechanical systems (MEMS). In addition, some models with the capability of controlling the wavefront polarization modes are also included herein since these are the base of hybrid transmitarrays, i.e., transmitarray with both electronic beamsteering and polarization control. Finally, all the models are compared against each other in order to highlight their benefits and limitations, summarizing their main characteristics, such as the frequency of operation and bandwidth, insertion loss, physical dimensions, and maximum beamsteering range, when available.

INDEX TERMS Antenna, beamsteering, beamforming, metamaterials, polarization, transmitarray.

I. INTRODUCTION

Antenna beamsteering is a very useful and desirable technique in any wireless communication system since it allow to dynamically adjust the antenna pattern and consequently enhance reception [1]. Such feature is crucial to some applications that require tracking of objects and adaptation to dynamic scenarios with multi-path and moving scatterers, e.g. base-station dynamic antenna alignment, wireless back-haul links auto-alignment due to pole swaying and twisting in the wind or mobile user tracking. Since such antenna systems is focusing their energy toward the receiver, it is increasing the useful received signal level and thus, lowering the interference level. I.e. an higher Signal-to-inference Ratio increases the capacity of the system and improves range and the coverage area.

The most traditional manner of implementing beamsteering is by using arrays of antenna [1]–[3]. However, the well-known design limitations particularly regarding to the feeding network implementation, lead to the introduction of alternative techniques to perform beamsteering. In 1986, *McGrath* firstly introduced in his paper [4] a microwave lens with focusing and scanning capabilities, by simply connecting two microstrip patch antennas using vias in both sides of a planar structure, forming a spatial array of microstrip patches, *i.e.* a transmitarray. Since then, transmitarray has been seen as a feasible alternative to phased antenna arrays and the focus of novel and extensive research nowadays.

Transmitarray [5]–[7] is the conventional name given to structures that can modify the original radiation pattern of a directional antenna source, *e.g.* horn antenna, when placed at a distance sufficiently away from the its aperture. To the set composed by the structure and the radiating source, it is referred as transmitarray antenna [5]–[7]. Due to their electromagnetic properties, such structures are be capable of modifying the characteristics of the incident Electromagnetic (EM) wave emitted by the source, and perform beamsteering, focusing or even polarization control, by re-transmission of the incident EM wave. Thus, one can imagine a transmitarray acting, in a sense, like a lens, allowing to pass-through the incident wave with an alteration (or not) of its direction of propagation, as depicted

The associate editor coordinating the review of this manuscript and approving it for publication was Chan Hwang See.

This work is licensed under a Creative Commons Attribution 4.0 License. For more information, see http://creativecommons.org/licenses/by/4.0/

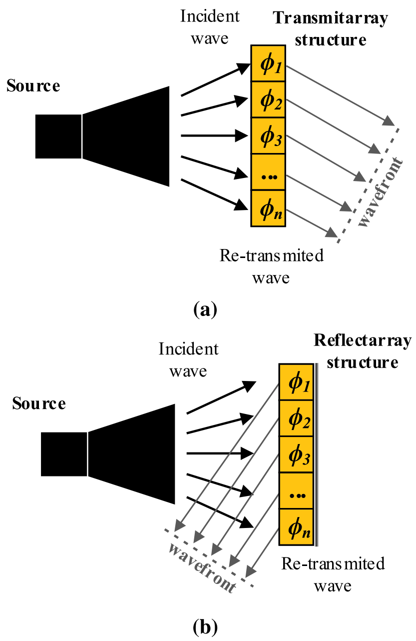

FIGURE 1. Generic model of (a) a transmitarray and (b) a reflectarray antenna.

in Fig. 1a. The direction to which the incident wave is being re-radiated depends on the design of the structure. These structures are commonly composed by several resonant unitary elements (unit-cells) with a spatial periodicity forming a planar array [5]–[7]. The unit-cells are typically based on simple microstrip patches, or inspired by metamaterials (MM) [8], [9] and frequency selective surfaces (FSS) [10]–[13]. From a practical point of view, since transmitarray structures are mostly implemented using Printed Circuit Board (PCB) technology [5]–[7], by etching the unit-cell geometries on a copper covered substrate, they benefit from being planar and thus easy to integrate with other peripherals. Furthermore, they are compatible with Surface Mount Technology (SMT) allowing to reduce the size of assemblies, and finally, since they have the electromagnetic feeding source separated from the beamsteering network, they offer higher degree of modularity to the system as opposed to traditional antenna array. Thus due to their design simplicity and, more importantly, due to the low manufacture costs, they have been extensively utilized for numerous antenna applications.

In order to achieve reconfigurability and enable features, such as electronic beamsteering, polarization control or frequency tuning, transmitarray are typically enhanced by using p-i-n diodes, varactor diodes, radio frequency (RF) or microelectromechanical-systems (MEMS) switches or manufactured using tunable substrates as liquid crystal or graphene. However, each of these methods present advantages and disadvantages, *e.g.* p-i-n and varactor diodes are widely utilized in transmitarray designs from low RF to around 30 GHz, mostly due to their size, easy integration in PCB and low cost. However, they are limited when operating at high frequencies (above 30 GHz), with insertion loss proportional to the frequency of operation that arise from their intrinsic parasitic parameters (series resistance, capacitance and inductance). RF and MEMS switches are typically more expensive than p-i-n/varactors and prone to failure over time, due to the wear and tear of the mechanical parts. Alternatively, tunable dielectric materials, *i.e.* materials that can have their electromagnetic properties (in particular ϵ_r) manipulated by an external stimulus (bias or voltage), such as liquid crystal and graphene are also employed for transmitarray implementations [14]–[20]. Furthermore, while liquid crystal technology have been successfully employed in transmitarray designs [14], it is more commonly used in reflectarray implementations [21]–[24] or as grounded substrate for conventional microstrip antennas [25]–[27]. Graphene substrates, on the other hand, are typically used at THz frequencies due to their unique electronic properties as reported in [28], even though applications in antennas design at micro- and millimeter-wave frequencies, have already been reported in [29].

The research on transmitarray has always been paired to the one on reflectarray [30], [31]. Reflectarray, which operating principle is depicted in Fig. 1b, makes use of the reflection principle (based on Snell's law [30], [31]) to modify the properties of the re-transmitted EM wave. In fact, the most significant difference between a transmitarray and reflectarray is that, in the latter, all power is re-radiated independent on the frequency or cell design. If the unit-cells are not matched to the frequency of operation, the elements will have small effect on the array response and the reflecting ground plane will predominate. In the worst case scenario, the reflected wave could have the same direction of the original one [30], [31]. On the other hand, for a transmitarray, if the structure is not well matched to the free-space or if the unit-cells are not adapted to the frequency of operation, the incident EM wave will be totally reflected back, resulting in no transmission through the structure [5], [6]. Therefore, a transmitarray is desirable to be the most ''transparent'' as possible, introducing very low loss so the EM field of the propagating wave is not severely attenuated, whereas the reflectarray is desirable to be a perfect reflecting surface so the incident wave can be entirely reflected.

However, although reflectarray have been successfully implemented in [7], [30]–[36], the feed blockage remains a challenge in implementation of such type of devices since the feeding source is on the same side of the radiated field. This may be a challenging depending on the final application that can be overcome with the use of a transmitarray.

To this extent, this paper presents an overview of the literature on transmitarray aiming antenna beamsteering. It starts by introducing the theoretical background for antenna beamsteering using a transmitarray. In particular, the mode of operation of 1 dimensional (1D) and 2 dimensional (2D) beamsteering with a transmitarray are described. Subsequently, a dedicated review based on several journal and conference publications, is presented. The overview presents a critical analysis on several electronically reconfigurable

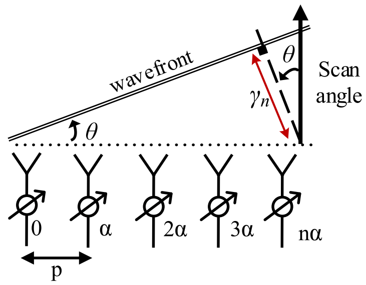

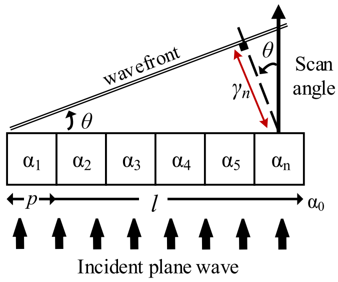

FIGURE 2. (a) Model of linear antenna array and (b) model of a transmitarray for 1D beamsteering analysis.

transmitarrays for antenna beamsteering, based on microstrip patch, FSS or MM, employing either p-i-n diodes, varactor diodes or MEMS switched to achieve reconfigurability. In addition, several transmitarray models with polarization control capabilities are also included in this paper yielding to the introduction of hybrid transmitarray, with both electronic beamsteering and polarization control capabilities. Finally, the most relevant transmitarray designs proposed by several authors are compared against each other in order to highlight its benefits and limitations. Their main characteristics such as frequency of operation and bandwidth, insertion loss, physical dimensions and maximum beamsteering range, are then summarized.

The paper is organized as follows: section II presents the mathematical ground for beamsteering with a transmitarray; Section III outlines the state of the art on Transmitarray covering in particular transmitarray for antenna beamsteering, polarization control and hybrid transmitarray, that enable both features simultaneously. Finally, the main conclusions are drawn in section IV.

II. BEAMSTEEERING WITH A TRANSMITARRAY

A. THEORETICAL MODEL FOR 1D–BEAMSTEERING

The principle of beamsteering using a traditional transmitarray can be compared to the one using a linear antenna array. Figure 2 depicts both configurations for comparison. In a linear antenna array, the phase shifting is applied to the signal in each individual branch using a phase shifter [1]–[3], whilst in a transmitarray the phase shifting is obtained by controlling the phase delay introduced by each individual elements of the transmitarray, as reported in [5]–[7], [37]–[56].

When an incident Electromagnetic (EM) wave propagates through a transmitarray of length l, composed by N elements of periodicity p (Fig. 2b), it experiences a different phase shifting γ_n expressed by (1), after penetrating each of the elements of the array in the steering direction theta (θ),

$$\gamma_n = \frac{2\pi}{\lambda_0}.p.n.sin\theta = k_0.p.n.sin\theta, \tag{1}$$

where $k_0 = \frac{2\pi}{\lambda_0}$ is the wave number in free space.

Consequently, the transmission phase α_n in the n^{th} element, can be defined by (2),

$$\alpha_n = -\gamma_n + \alpha_0 + 2\pi i, \quad i = 0, 1, 2, \ldots \tag{2}$$

where α_0 is the phase of the incident EM wave at the input of the transmitarray.

Therefore, the re-transmitted wave direction θ can be expressed as a function of the phase difference ψ between adjacent elements, *i.e.* progressive phase, using (3),

$$\begin{aligned} \psi &= \alpha_n - \alpha_{n-1} = -\gamma_n + \gamma_{n-1} \\ &= -k_0.p.n.sin\theta + k_0.p.(n-1).sin\theta \\ &= -k_0.p.sin\theta. \end{aligned} \tag{3}$$

Thus, by varying the phase α_n of each array element in a progressive way, the incident wave can be steered to a desired direction θ relative to the normal of the structure, defined by (4),

$$\psi = -k_0.p.sin\theta \Leftrightarrow \theta = -sin^{-1}\left(\psi.\frac{\lambda}{2\pi.p}\right) \tag{4}$$

However, since the phase distribution in the array is applied along a single direction only, the model for a linear transmitarray limits its application to 1D beamsteering. Therefore, the main lobe of the radiation pattern of the original antenna in which the transmitarray is applied, only has the capability to be steered towards the output angle with θ component, as reported in some of the references included in the literature review [14], [37]–[39], [47], [48], [52], [53].

B. THEORETICAL MODEL FOR 2D–BEAMSTEERING

In order to extend the concept to 2-D beamsteering using a transmitarray, it is proposed herein to characterize the model by analogy with a planar antenna array. This vision enable the transmitarray to have the control over the two angular components theta (θ) and phi (ϕ) of the output angle direction, simultaneously, raising the limitation of 1D beamsteering of the previous model. The transmitarray model for 2D beamsteering is depicted in Fig. 3.

Built on the theory of planar antenna arrays, presented in [1] and [3], a progressive phase shift between adjacent elements should occur along the X and Y directions of the $M \times N$ array so 2D beamsteering could be enabled. Thus, by expanding from (3), the relation between the two dimensional output directions (θ,ϕ) and the progressive phase delay,

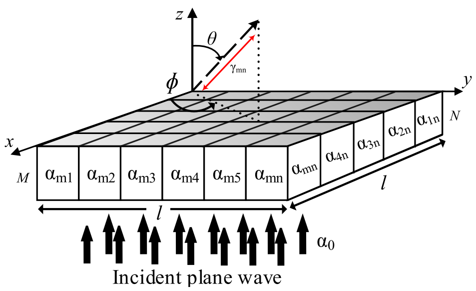

FIGURE 3. Proposed model for a transmitarray with 2D beamsteering.

is given by (5),

$$\begin{cases} \psi_x = -k_0.p.sin(\theta).cos(\phi) \\ \psi_y = -k_0.p.sin(\theta).sin(\phi), \end{cases} \tag{5}$$

where ψ_x and ψ_y are the progressive phase along X and$Y$ axis, respectively, and p is the periodicity of the $p \times p$ array elements.

Therefore, a $M \times N$ transmitarray would exhibit a relative phase distribution that can be represented by the matrix (6),

$$\begin{matrix} & \longrightarrow \psi_x \\ \psi_y \downarrow & \begin{bmatrix} \alpha_{1,1} & .. & .. & .. & .. & \alpha_{1,n} \\ .. & .. & .. & .. & .. & .. \\ .. & .. & .. & .. & .. & .. \\ \alpha_{m,1} & .. & .. & .. & .. & \alpha_{m,n} \end{bmatrix} \end{matrix} \tag{6}$$

where $\alpha_{m,n}$ is the phase delay introduced by each individual (m,n) element of the transmitarray. This representation is proposed herein to facilitate the understanding of the progressive phase along the transmitarray and will be further considered herein.

From this analysis, it can be concluded that the output steering direction (θ,ϕ) depends on the transmission phase $\alpha_{m,n}$ of each element of the 2–D transmitarray, and similarly to (2) (linear case), the phase shifting in each individual element can be described by (7),

$$\alpha_{m,n} = -\gamma_{m,n} + \alpha_0 + 2\pi i, \quad i = 0, 1, 2, \ldots, \tag{7}$$

where the phase shifting of each element $\alpha_{m,n}$ is a periodic function, and $\alpha_{m,n} \subset [0, 2\pi]$ such as in the 1-D case. Thus, each element of the transmitarray must always be capable to achieve at least 360° (2π) of transmission phase shift, to ensure a complete control of the output angle.

Notwithstanding, in order to directly match the output angle direction obtained from the theory with the output angle direction given either by simulation and experiments, it is proposed, by this work, to apply in the theoretical model a coordinate system conversion from Spherical coordinates (represented by θ and ϕ components) to *Azimuth-over-Elevation* (represented by the pair *Az/El*). Therefore, the mathematical relation between spherical and *Az/El* coordinates well detailed in [57], given by (8), has been applied here:

$$\begin{cases} sin(\theta).cos(\phi) = cos(El).sin(Az) \\ sin(\theta).sin(\phi) = sin(El). \end{cases} \tag{8}$$

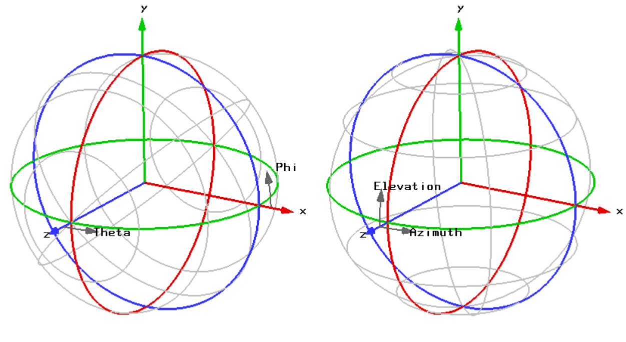

(a) (b)

FIGURE 4. Axial representation of the (a) spherical coordinate system (θ/ϕ) and (b) *Azimuth-over-Elevation* coordinate system (*Az*, *El*).

The main differences between both coordinate systems rely on the origin of the axis, as depicted in Fig. 4. From the mathematical workout resultant of replacing (8) in (5), a generic formula to calculate the output angle direction with *Az/El* components provided by a 2D transmitarray, is given by (9),

$$\begin{cases} \psi'_x = -k_0.p.cos(El).sin(Az) \\ \psi'_y = -k_0.p.sin(El). \end{cases} \tag{9}$$

III. STATE-OF-THE-ART ON TRANSMITARRAY ANTENNAS

A. TRANSMITARRAY FOR ANTENNA BEAMSTEERING

Several examples can be found in the literature for transmitarray aiming antenna beamsteering. They comprise the use of different materials, unit-cells designs and implementation approaches. However, there is one requirement that must be satisfied to use such structures to steer the main beam of an antenna radiation pattern. The unitary element that composes the transmitarray must have transmission phase that can be varied (tunable) up to 360° (as mentioned in section II-B), while the transmission magnitude (desirably) remains constant over the bandwidth,. Therefore, this section is focused on the review of transmitarray structures and unit-cell elements, with reconfigurable capabilities that enable electronic beamsteering.

1) RECONFIGURABLE BASED ON MICROSTRIP PATCHES

Particularly in [37], a reconfigurable transmitarray for beamsteering is proposed. The device is composed of a set of patch antennas placed on each side of the array structure and connected by an electronically tunable phase-shifter, where the innovation of the work relies on. The phase-shifter is developed in transmission line technology and consists of a microstrip directional coupler terminated with reflective LC circuits, whose capacitance (C) is controlled by a varactor diode. Consequently, by tuning the value of C, it is possible to selected whether the terminations of the coupler are open- or short- circuit and thus, control the phase-shift between the input and the output of the transmitarray. Nevertheless, this solution turned out to be limited in terms of phase range

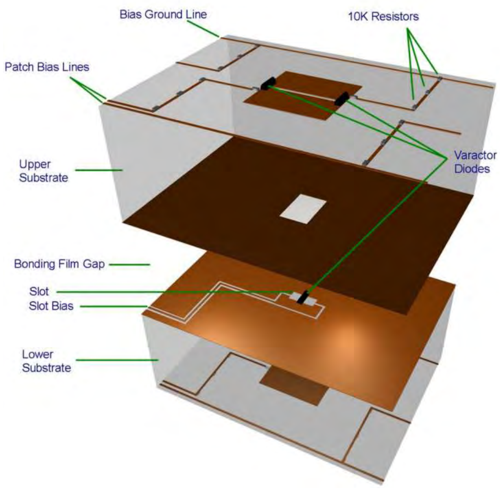

(a)

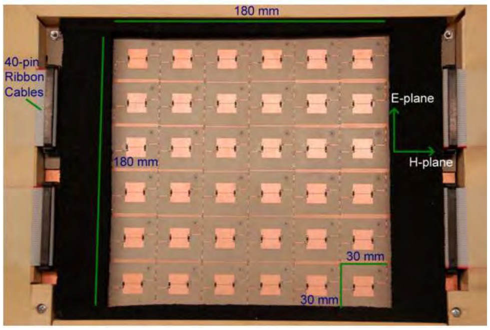

(b)

FIGURE 5. (a) Reconfigurable element (exploded-view) and (b) respective transmitarray prototype (images extracted from the work presented in [39]).

and since several couplers are cascaded together to overcome this issue, the size and complexity of the phase-shift network is consequently increased. This forced a large separation between the radiating elements, that were arranged in groups of 4 elements and separated by 1.4 wavelengths, leading to the reduction in the scan capability and to the appearing of grating lobes. Therefore, a maximum of 9° of angular shift is reported on the azimuth plane. The proposed solution presents 700 MHz of bandwidth and 3 dB of insertion losses but such values are advertised for the phase-shifter alone and not for the complete transmitarray.

Remarkably in their work, *Lau* and *Hum* [5], [38]–[41] have introduced several models of active unit-cells and of electronically controlled transmitarray. Specifically aiming antenna beamsteering, it is presented and characterized in [38] and further improved in [39] a transmitarray element (Fig. 5a) that consists of two microstrip patches on either side of a ground plane coupled to a small slot aperture. Each patch is split in half with a small gap in between, and varactor diodes inserted to connect the two halves, while another varactor diode is inserted at the center of the slot, connecting the two sides of the slot. Together, all these parts act as three coupled tunable resonators that provides a variable phase-shift over 360° with 3 dB of insertion losses, as reported in [39]. However, the losses are slightly increased to 4.8 dB (over the same bandwidth), when the proposed element is composing a 6×6 array and the biasing network to control the varactors are included, as depicted in Fig. 5b [39]. Nonetheless, the developed prototype achieved $\pm 25°$ of electronically controlled beam scanning, in azimuth and elevation planes independently, with a broadside directivity of 20.8 dBi.

As alternative, a different unitary element is proposed and characterized by the same authors in [40]. The unit-cell for transmitarray applications explores the properties of proximity-coupled feeding and aperture coupling [1]. In this solution, the array element is implemented with microstrip patches in both sides of the structure separated by a ground plane. Each patch fed a differential microstrip transmission line by mutual coupling. In one of the sides, possess a differential bridged-T phase-shifter composed by varactor diodes and DC blocking capacitors. Both sides of the structure are further interconnected also by aperture coupling through two open slots etched in the ground plane. According to experiments realized on a single unit-cell using the waveguide method, which consists of a sample of the unit-cell enclosed between two waveguide flanges, it is notably achieved a tunable phase range of around 425° and insertion loss in average of 3.4 dB at 4.86 GHz. This model is however limited by the narrow bandwidth of the radiating elements and such drawback is mitigated, on a final prototype by employing a stack of microstrip patches. The final array element exhibits insertion losses of around 3.6 dB with a phase range over 400°, but the bandwidth was increased from 100 to 500 MHz at the same central frequency. Subsequently, a 6×6 reconfigurable transmitarray composed of active elements of [40] is finally presented and evaluated in terms of beamsteering performance in [41]. The prototype of the transmitarray provides a scanning range of $\pm 50°$ in both elevation and azimuth planes, with 2.2 dB of insertion losses and 10% bandwidth (500 MHz) at 5 GHz.

Moreover, in [42], a novel unit-cell design is proposed and characterized for an electronic control of the wave direction using a transmitarray. It is composed of a passive microstrip patch antenna with U-shape slot etched on the reception plane, and an active patch with an etched O-shape slot in the re-transmission plane, as depicted in Fig. 6a. The active O-shape is loaded with two p-i-n diodes (and in an alternative design with RF- MEMS) that allow to control the transmission phase by alternatively activating diode states. A 15% of bandwidth and around 3 dB of insertion losses at 10 GHz are reported experimentally on a single unit-cell, evaluated using the waveguide method also employed in [40]. Later in [43], the same unit-cell design using MEMS presents a bandwidth of 16% but 4 dB of insertions losses. In [44] the authors presented a full characterization of a 20×20 transmitarray comprising 800 p-i-n diodes and the respective feeding mesh. The prototype is depicted in Fig. 6b. The authors state that the

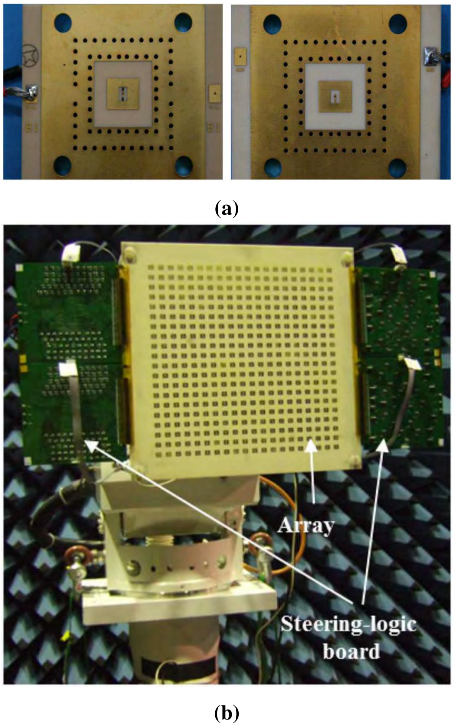

FIGURE 6. (a) Unit-cell design and (b) transmitarray prototype for antenna beamsteering (images extracted from the work presented in [42] and [44], respectively).

proposed transmitarray exhibits a 2D beamsteering capability with maximum ranges of ±40° in elevation and ±70° in azimuth.

Another unit-cell for beamsteering transmitarray at Ka-band based on p-i-n diodes is presented in [45]. The paper starts by characterizing by simulations a novel unit-cell design. In particular, this novel unit-cell design allows for a 2-bit phase resolution and has an overall size of $5.1 \times 5.1 \times 1.3\ mm^3$ ($\lambda/2 \times \lambda/2 \times \lambda/8$ at 29 GHz). The unit-cell is composed of six metal layers printed on three substrates as shown in Fig. 7b, of which the ones at the edges are O-slot rectangular patch antennas loaded with two p-i-n diodes for phase control. Similar to other cases already presented [42], [44], the p-i-n diodes in each of the antennas are biased in opposite states (one p-i-n diode is ON while the other is OFF). By choosing which diode is ON at a given time, a 180° phase-shift is achieved. Therefore, by combining the different states of the receiving and transmitting layers, a total of four phase shifts can be achieved (0°, 90°, 180° and 270°). The presented unit-cell is used to implement a 14×14 element transmitarray in simulation environment whose beamsteering range is reported up to −40°, as shown in Fig. 7b.

More recently, in [46] a new unit-cell for a beamsteering transmitarray is presented. Each cell is comprised of four stacked Rogers RO4350B double sided layer, as depicted in Fig. 8a. Since one pair of layers (sub-element) can only achieve 180°, this arrangement has to be replicated in order to achieve the desired 360° of phase shift. Varactor diodes are used in every layer to control, electronically,

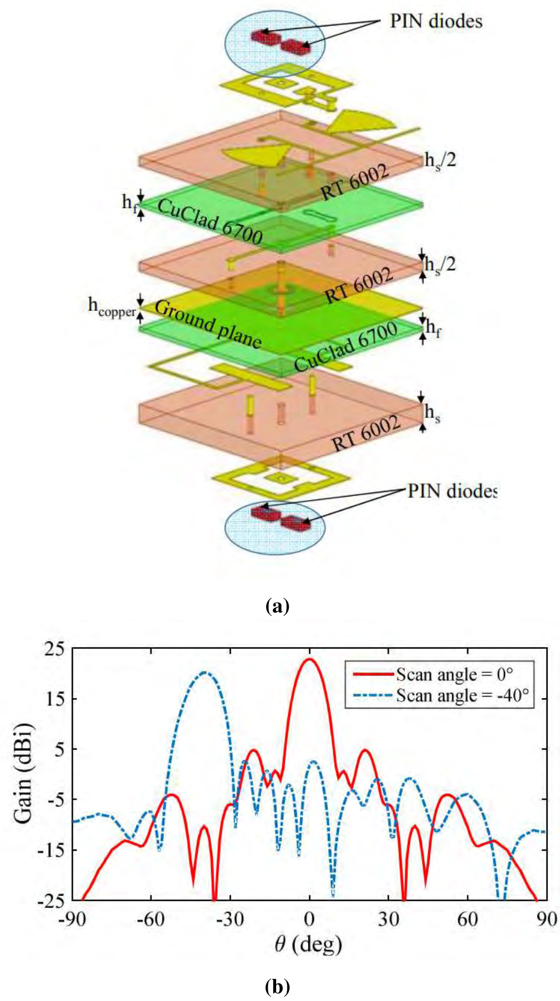

FIGURE 7. (a) Schematic view of the 2-bit unit-cell and (b) simulated radiation pattern for two angles (images extracted from the work presented in [45]).

the element phase-shift. Although the paper reports a bandwidth of 1 GHz for the unit-cell at 24.6 GHz, this value is defined by the frequency range in which the phase-shift is above 360 degrees, and not from the S_{11}/S_{22} filtering response as normally characterized in this type of work. This unit-cell, exhibits then a total insertion loss of around -5 dB obtained in simulation and -12 dB obtained experimentally. Finally in [46] a 6×6 transmitarray composed of the aforementioned unit-cell has been built (Fig. 8b). This transmitarray is able to steer the main beam direction up to ±50° in both the azimuth and elevation planes, at 24.6 GHz, with a maximum attenuation of 17 dB at the extremes of the steering interval.

2) RECONFIGURABLE BASED ON TUNABLE METAMATERIALS

Transmitarray composed of metamaterials (MM) to perform antenna beamsteering are also reported in the literature. Metamaterials are artificial man-made structured materials able to produce electromagnetic properties

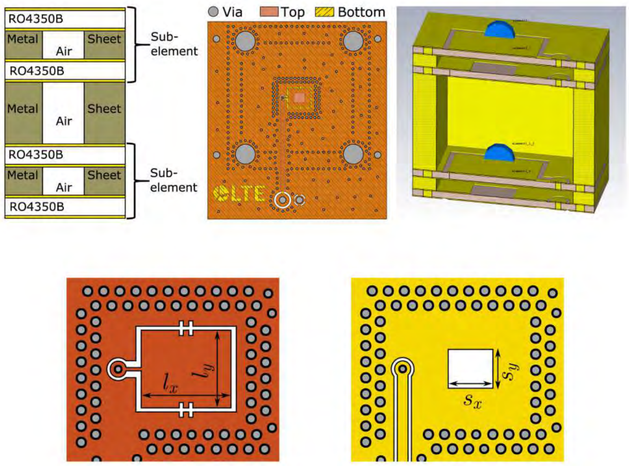

(a)

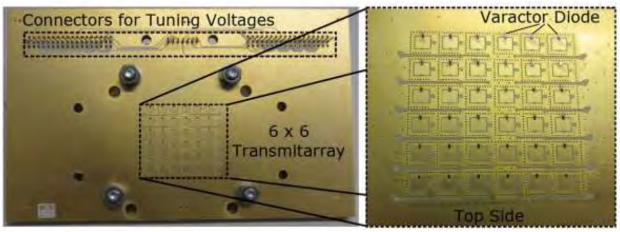

(b)

FIGURE 8. (a) Unit-cell design and (b) top view of assembled 6 × 6 transmitarray prototype (images extracted from the work presented in [46]).

(permittivity, permeability and refractive index) which are unusual or non-existent in nature [8], [9] and such properties can be explored for transmitarray designs.

It is the case of the work described in [14], [47] and [48], where 1D beamsteering, *i.e.* main lobe limited to steering in a single plane, is demonstrated using such type of materials. These works [14], [47], [48] suggest new steerable antennas by using controllable MM (electronically reconfigurable) to form the transmitarray. Although implemented with different resonant unit-cell designs, they all respect the same physical principle: tunable refractive index structures are utilized to electronically control the direction of the outcoming wave. The steering is achieved when the refractive index of the MM structure is tuned, leading to a progressive phase distribution along the structure, acting as a linear phased array.

For example, in [14] the authors have developed and characterized an artificial gradient-index metamaterial by designing a fishnet structure on a liquid crystal substrate. The transmitarray was practical validated against measurements conducted at 27.5 GHz. A beamsteering angular range limited to ±5° was achieved by varying, in a gradient manner, the bias of each array column. According to the authors, the yielded angular range can be enhanced by staking more layers of the one depicted in Fig. 9.

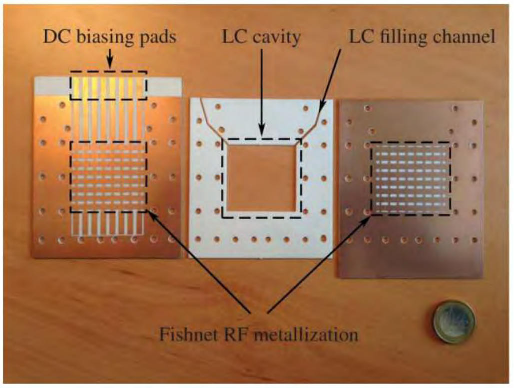

FIGURE 9. Prototype of a single opened fishnet unit-cell layer (images extracted from the work presented in [14]).

In [47] and [48], the authors have followed an alternative approach to design their transmitarray. Both presented structures are composed of staked layers of periodically printed sub-wavelength metallic resonators with embedded microwave varactors. By adjusting the varactor diode, the resonant characteristics of the unit-cell is modified controlling, in fact, the associated phase-delay between the first and the last layer of the transmitarray. Consequently, the associated effective refractive index of a single transmitarray element is being adjusted. Accordingly, if a progressive phase between adjacent elements is applied through the array in order to perform beamsteering, the metamaterial exhibits a gradient index of refraction, when seen as a whole.

Therefore in [47], 6 stacked layers of a double-layer I-shaped unit-cell (Fig. 10a) are suggested as array element, exhibiting 360° of phase-shift at 1.6 GHz while the varactor is tuned from 0.1 pF to 1.9 pF, with insertion losses of 4 dB (averaged). Bandwidth is not referred by the authors. A continuous scanning range of ±30° in the azimuth plane is achieved using a full wave simulator. Although it is stated that experimental results obtained on a prototype are consistent with simulation ones, the paper lacks a more elaborated and physically grounded analysis of the results.

Notably in [48], a complete characterization of a metamaterial transmitarray composed by the unit cell presented in Fig. 10b was performed. In addition to the transmitarray, an array of microstrip patch antennas was also developed to serve as feeding source. The prototype, implemented on a stacked layer structure (Fig. 11a), presents an angular steering range of ±30° in azimuth verified under experiments at 4.7 GHz. Some samples of radiation pattern are demonstrated by the authors in their paper and illustrated in Fig. 11b.

Although introduced as metamaterials by analyzing the refractive index of the array element, it can be noticed that such structures are in fact frequency selective surfaces. While the unit-cell presented in [47] exhibits a low-pass filtering frequency response, the unit-cell of reference [48] possesses a band-pass filtering type. Herein, is when the term metamaterials could be misleading due to large ambiguity of the definition.

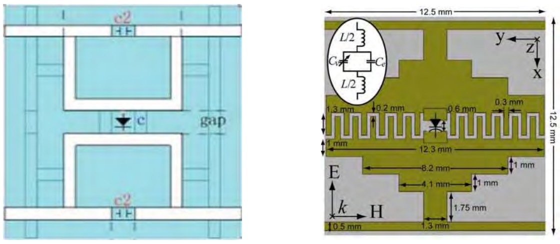

(a) (b)

FIGURE 10. **Metamaterial unit-cells for transmitarray antennas presented by (a) *Yongzhi S. et. al.* and by (b) *Jiang T. et. al.* (images extracted from the work presented in [47] and [48], respectively).**

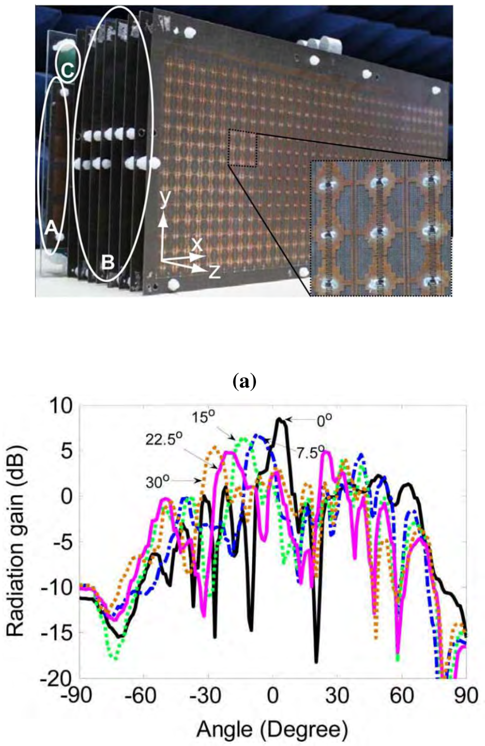

(b)

FIGURE 11. **(a) Prototype of the MM beamsteering antenna and (b) measured radiation pattern for different steering angles (images extracted from the work presented in [48]).**

3) RECONFIGURABLE BASED ON FSS

Frequency selective surfaces [10]–[13] are, per se, a timely topic on the field of (antennas and) propagation that have been studied for years. A FSS is a spacial filter that exhibits distinct resonant filtering characteristics *e.g.*: band-pass, band-stop, high-pass or low-pass, that depend on the format and on the dimensions of periodic resonant geometries etched over a metallic coated substrate [10]–[13]. As a spacial filter, these structures are able to allow or block the propagation of an incident EM wave within a specific frequency band and even control its propagation phase.

Much of the work about FSS relies on the study and development of novel unit-cell designs for EM blockage (shielding) or radio coverage enhancement [10]–[13]. However, new applications have recently emerged by exploring the use FSS in various transmitarray implementations [49]–[56], [58] and in novel antenna designs [59]–[61].

For example in [58], a wide-band transmitarray is suggested by using a FSS of double square rings unit-cells. The authors have demonstrated that the phase-shift introduced by the transmitarray can be varied by simply modifying the physical size of the squares, and such can be further improved by stacking several layers of FSS on top of each others. In fact, the concept of stacked layers separated by an air gap is widely used for transmitarray implemented with FSS since it allows to increase both the bandwidth and the transmission phase of the structure, as thoroughly reported in [5], [51], [54], [55], [58].

In particular, some examples can be found in [49]–[53] by presenting reconfigurable transmitarray of FSS for antenna beamsteering. The majority of the work utilizes varactor diodes to electronically control the capacitance of the equivalent LC circuit that characterizes the resonant unit-cell design, as presented by *Russo et. al.* in [49]–[51]. In their work, a tunable pass-band FSS suitable for beamsteering operations is proposed. The suggested FSS, depicted in Fig. 12a, is evaluated by simulations in [49], [50] and experimentally characterized in [51], also using the waveguide method (Fig. 12b), previously described. The proposed structure is capable of bandwidths ranging from 1% to 10% (with a few modifications in original design) at 4 GHz, with a transmission amplitude that remains above 3 dB within the varactor tuning range. Although the transmission phase obtained from experiments varies by approximately 360° over the whole bandwidth, making this design suitable for beamsteering, the paper does not include the implementation of a complete transmitarray and respective beamsteering characterization.

In [52], an active FSS based on the traditional squared-slot design with band-pass filtering characteristics is implemented for antenna beamsteering, as depicted in Fig. 13. Varactor diodes are used to tune the FSS and control the phase-shift, with range up to 360°, of a structure composed of 5 stacked layers. In fact, the authors have demonstrated on a physical prototype, illustrated in Fig. 13a, that through different configurations of the bias voltages applied to the varactors, a gradient phase distribution along the transmitarray can be utilized to steer the radiation pattern of a horn antenna. This corroborates with the facts presented for MM transmitarray introduced in last section. Although the work show its merits by presenting a tunable steering range of ±30° in both azimuth and elevation plans at 5.3 GHz, as depicted in Fig. 13b and Fig. 13c respectively, it is a fact that such scanning angle can only satisfy one steering direction at the time. Therefore, two-dimensional beamsteering, *i.e.* steer the main lobe to a direction with two spatial components as presented in Section II-B, is still unachievable with this device.

Alternatively in [53], a tunable FSS with beam steering capability is presented. The FSS is used as a transmitarray with a bandpass characteristic centered at 12 GHz.

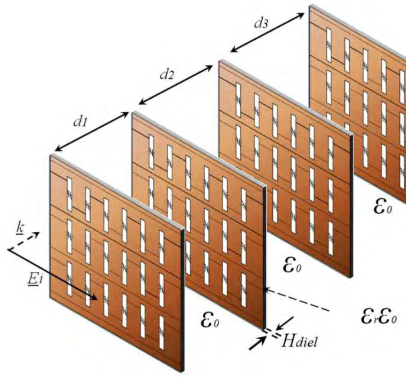

(a)

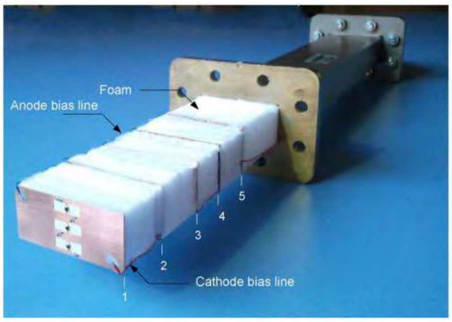

(b)

FIGURE 12. **(a) FSS transmitarray model and (b) respective unit-cell prototype evaluated using the waveguide method (images extracted from the work presented in [50] and [51], respectively).**

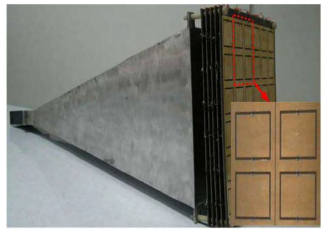

(a)

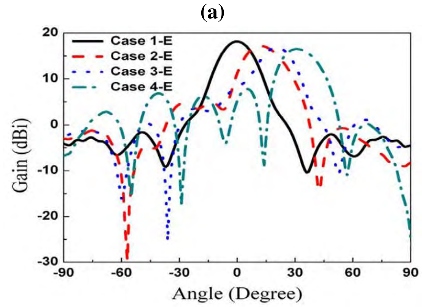

(b)

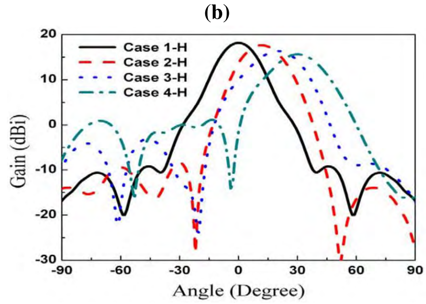

(c)

FIGURE 13. **(a) 6 × 6 transmitarray prototype, (b,c) measured radiation pattern in azimuth and elevation planes, respectively (images extracted from the work presented in [52]).**

The novelty of the work relies on the FSS design which is composed of capacitive (parallel electrodes) and inductive (vertical wires) structures printed on a BST thick-film ceramic, as illustrated in Fig. 14. The tunability is performed due to the properties of the BST substrate that can be tuned by applying an external electrostatic field across the material, and not by using discrete components such varactors or p-i-n diodes. By applying a DC field between the electrodes of the capacitor, the effective permittivity is reduced resulting also in a capacitance reduction. Experiments realized on a 40 × 40 FSS transmitarray (Fig. 14b), report a maximum phase difference of 121° at 12 GHz when the bias voltage is ranging from 0 V (untuned state) and 120 V (maximum tuning state). Within such voltage range, the main beam of a feeding horn antenna is steered up to ±10° in the azimuth plane, due to the low phase-shift (121°) produced by the structure. Although showing its merits, the proposed solution is one of a type in the literature, possible due to the impractical voltage values necessary to apply for tuning the structure and perform beamsteering limited 1-Dimension, in comparison with other state-of-the-art proposals.

To withdraw such limitation, our research group has been working on a reconfigurable transmitarray model for 2D beamsteering. The transmitarray follows the phase distribution proposed by the theoretical model presented in section II-B in order to enable antenna beamsteering in two dimensional planes. With this mindset, it is presented in [54] and further in [55] the characterization of a FSS transmitarray with controlled beamsteering output direction in the two main antenna planes (azimuth and elevation). Firstly in [54], the theoretical model for 2D beamsteering has been applied on a passive stacked-layer FSS inspired

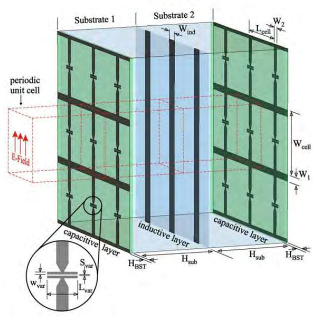

(a)

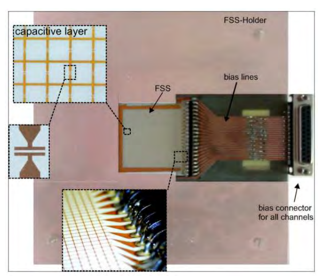

(b)

FIGURE 14. **(a) FSS transmitarray model and (b) respective transmitarray prototype (images extracted from the work presented in [53]).**

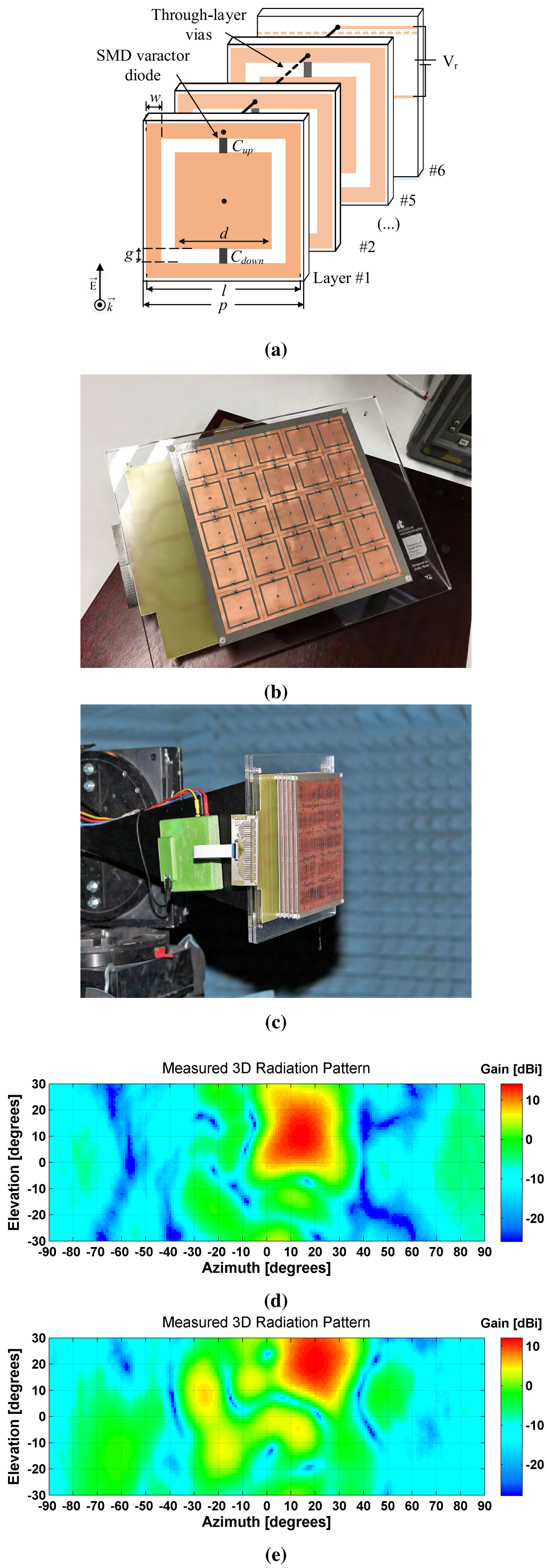

FIGURE 15. (a) Unit-cell model, (b,c) 5 × 5 transmitarray prototype and (d,e) measured radiation pattern for (+15°,+15°) and (+25°,+25°), respectively. (images extracted from [55]).

transmitarray. Based on a square-slot pass-band unit-cell layout (as in [52]), the 2D beamsteering model was tested for several beamsteering angles on a 5 × 5 transmitarray with

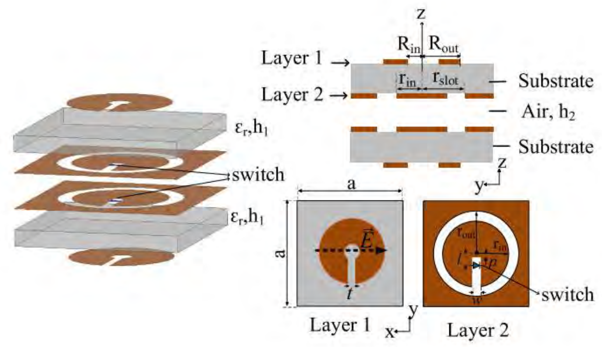

FIGURE 16. Geometry of transmitarray unit-cell (image extracted from the work presented in [56]).

5 stacked layers separated by an air gap, at 5.35 GHz. The paper, which also includes a parametric study to evaluate the ideal layer separation distance and the ideal number of layers necessary to achieve a desired phase-shift, reports beamsteering angles up to ±25° in both elevation and azimuth planes with 3° of error between simulation and experimental validating the theoretical 2D model. Although beamsteering is set by the value of each of the 50 discrete SMT capacitor loaded in each layer, the several output angles were achieved by hand-soldering the capacitors for each angular configuration.

Subsequently in [55], the latter model has been improved to enable electronically reconfigurable beamsteering. In the addition to through-layer *vias* per unit-cell, a sixth layer has been added to accommodate the feeding network, as depicted in Fig. 15a. Varactor diodes replaced the discrete SMT capacitors used in the passive transmitarray of [54]. A beamsteering driver has been developed to control, individually, the overall capacitance value of each of the 25 cells of the transmitarray. As result, beamsteering angles up to ±28° in azimuth and ±26° in elevation have been accomplished with the physical prototype of Fig. 15b. Two samples of measured radiation pattern are depicted in Fig 15d and Fig. 15e, for (+15°,+15°) and (+25°,+25°), respectively. The reconfigurable transmitarray exhibits insertion loss of 1.6 dB and 4.3 dB in simulation and experiments, respectively. This compares with the experimental results obtained in the passive model by presenting approximately 1.5dB of excess loss at 5.2GHz, due to the intrinsic parasitic effect of the selected varactor diodes.

Another design of FSS-based unit-cells for beamsteering transmitarray is presented in [56]. The unit-cell is based on a C-patch and ring slot loaded with p-i-n diodes (Fig. 16) and is composed of two identical substrates with dimensions of $14 \times 14\ mm^2$. The ring slot is loaded by a rectangular gap and is placed just beneath the gap of the C-patch. In this particular unit-cell, the C-patches act as the receiver and transmitter, while the ring slots act as a phase shifter. The phase shift between the receiver and transmitter can be controlled by modifying the length of the ring slot gaps. In order to change the associated electrical length, each gap is loaded with p-i-n

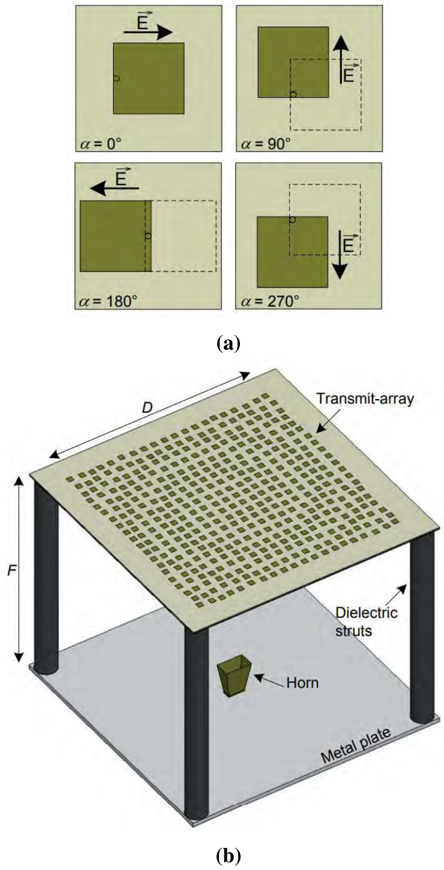

FIGURE 17. **(a) Patch unit-cell and (b) transmitarray model for polarization control (images extracted from the work presented in [63]).**

diodes that allow a 180° of phase shift at 11.5 GHz. However, since both terminals of the p-i-n diodes are short-circuited, a second rectangular gap was introduced in the cell presented in Fig. 16. This gap is 0.2 mm and is loaded with three 100 pF capacitors in order to the current flow through the gap. The first unit-cell was then simulated in a 12 × 12 transmitarray to verify its beamsteering capabilities. For each of the cells a single bias line is needed to control the ON/OFF state of the p-i-n diodes. Simulation results show that, at 11.5 GHz, a ±40° in both azimuth and elevation planes is achieved. At the moment there are not experiments on this structure.

B. TRANSMITARRAY FOR POLARIZATION CONTROL

Several transmitarray have been presented in last section all aiming antenna beamsteering. However, transmitarray have also been used to control the polarization of the re-radiated EM, as the ones described as follows.

First introduced in [62] and further in [63], the authors have presented a transmitarray with the objective of controlling the polarization of the wavefront. The proposed structure is based on microstrip patch antennas, whose elements in the outer side of the structure are physically rotated (α = 0°, 90°, 180°, and 270°) relative to the patch feeding point), to tilt the polarization of the re-transmitted wave. The implemented unit-cells and the respective transmitarray are depicted in Fig. 17 [63]. The polarization of the re-radiated wave is forced by tilting mechanically of each unit-cell enabling the developed transmitarray to produce a circularly polarized wave. Since the polarization control is performed through sequential rotation and no other mechanism was implemented to automatically modify the properties of the transmitarray, rather than mechanical movement, the suggested model is considered a passive device.

Following the same approach, a novel passive transmitarray was latter introduced in [64] by the same research group. This particular device exhibits an enhanced unit-cell also based on microstrip patch with etched corners. A prototype of the device measured a broadside gain of 22.8 dBi at the simulated frequency with a 3 dB bandwidth of 20% in Right-hand Cross Polarization RHCP and 3 dB axial ratio with bandwidth of 24.4%.

With a novel unit-cell design and following a slightly different methodology, a novel transmitarray was introduced by *Pfeiffer* and *Grbic* in [65]. This design was implemented by using cascading metallic surfaces to provide polarization and wavefront control. Two transmitarray were developed and tested experimentally both based on a quarter-wave plate design that transforms a linearly polarized incident wave into a circularly polarized transmitted wave, by exploring the phase shift created between both faces of the structures. Since the phase difference between two orthogonal E-field components is a quarter of the wavelength (90°), when an incident field is linearly polarized at (45°) relative to its axes, the quarter-wave plate converts the transmitted field to circular polarization.

In [66] another polarization controlled transmitarray has been presented by stacking together several layers of rectangle ring slot unit-cells, separated by an air gap. Remarkably, the proposed device is capable of realizing Left- and Right-hand cross polarizations (LHCP/RHCP), and linear polarization, when excited by a linearly polarized feeding source (*Vivaldi* antenna). This is achieved due to the enhanced phased control given by the stacked layers but also by varying the size of the unit-cell throughout the array. By varying the X and Y dimensions of the rectangle ring slot element, transmission magnitude and phase shift for both polarizations can be achieved. Therefore, it is possible to perform a change in polarization by adjusting the rotation angles of the feeding antenna through the phase of the linearly polarized incoming wave.

The main difference in the underlying principle between both physical rotated and phase delayed unit-cells is well detailed in [67]. The authors have presented a detailed comparison between both types of unit-cells through simulations and practical validation in two different transmitarray prototypes. Their study reveal that the transmitarray based on physically-rotated unit-cells exhibits wideband cross-polarization filtering characteristics, whereas the one with phase-shifted cells can offer polarization diversity (linear- and cross- polarization) with similar performance to

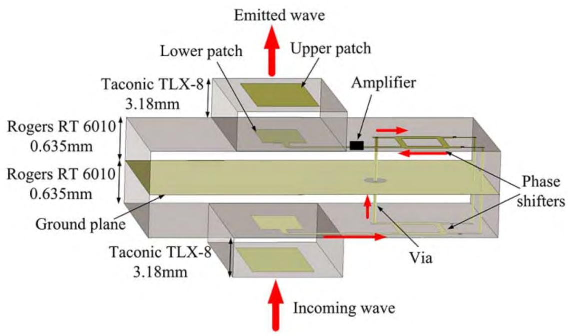

(a)

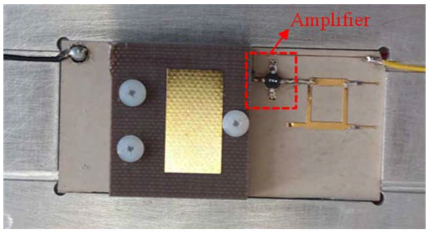

(b)

FIGURE 18. (a) Transmitarray unit-cell architecture and (b) photography of the unit-cell prototype (images extracted from the work presented in [73]).

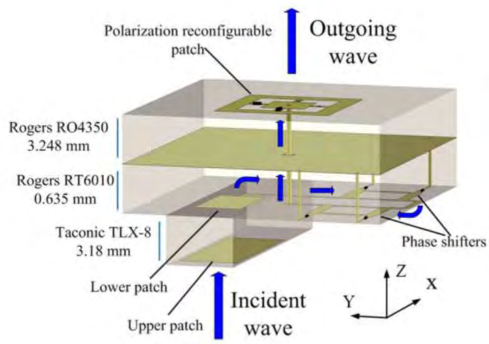

(a)

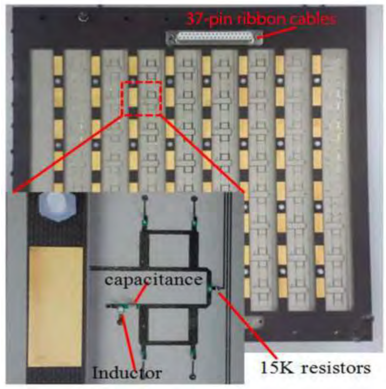

(b)

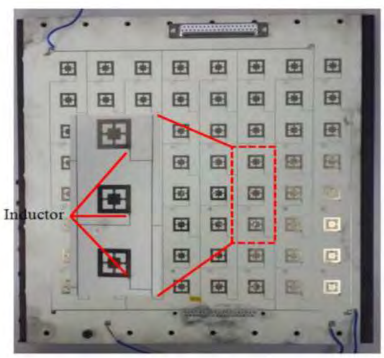

(c)

FIGURE 19. Transmitarray unit-cell architecture (image extracted from the work presented in [76]).

the former, but limited by 3 dB axial-ratio bandwidth and magnitude of the feeding antenna [67].

After analyzing the presented examples, both loss and bandwidth may be considered the two major challenges in the design of a transmitarray. Hence, consideration to this aspect should be given at the time of selecting the design layout for a transmitarray implementation, given the project specifications. For example, in FSS-type transmitarray, bandwidth can be easily increased at the expense of using several stacked layers, as already mentioned. However, the overall insertion loss will always be proportional to the total number of layers (and on the properties of the substrate) and, thus, difficult to compensate. On the other hand, transmitarray with unit-cells composed of microstrip patches commonly exhibit limited bandwidth typically associated to such structures [1], but the insertion loss can be reduced by using amplifiers placed between the inner and the outer faces of the transmitarray. In fact, this technique has already been reported in [68]–[75], but particularly in [73], a total average gain of about 7.7 dB is reported for experiments on the unit-cell of Fig. 18, overcoming the initial insertion loss of 2.6 dB experienced without any signal amplification.

C. HYBRID TRANSMITARRAY

Although the previous transmitarray designs [62]–[66] are not electronically reconfigurable (most are reconfigurable by mechanical rotation means), they yield to the development of hybrid reconfigurable transmitarray with both beamsteering and polarization capabilities.

It is the case of the reconfigurable transmitarray presented in [76] by *Huang, C. et. al.*. The authors have developed a transmitarray operating at 5.4 GHz with the capability of controlling electronically the polarization and direction of the re-radiated wave. Each unit-cell of the transmitarray is composed of several PCB layers separated by three different substrates, as depicted in Fig. 19. The face in which the electromagnetic wave is incident (Rx cell), a two-layer stacked patch is adopted. After being received by the Rx cell, the RF signal passes by two cascaded reflection type phase shifters and is coupled to the Transmitter cell (Tx cell) through a metallized via hole. Each of the phase shifter implemented integrate a four-port directional coupler and each port is loaded by a varactor-based tunable circuit in order to achieve the 360° phase tuning range. The Tx cell is made of a square patch with an O-slot structure loaded

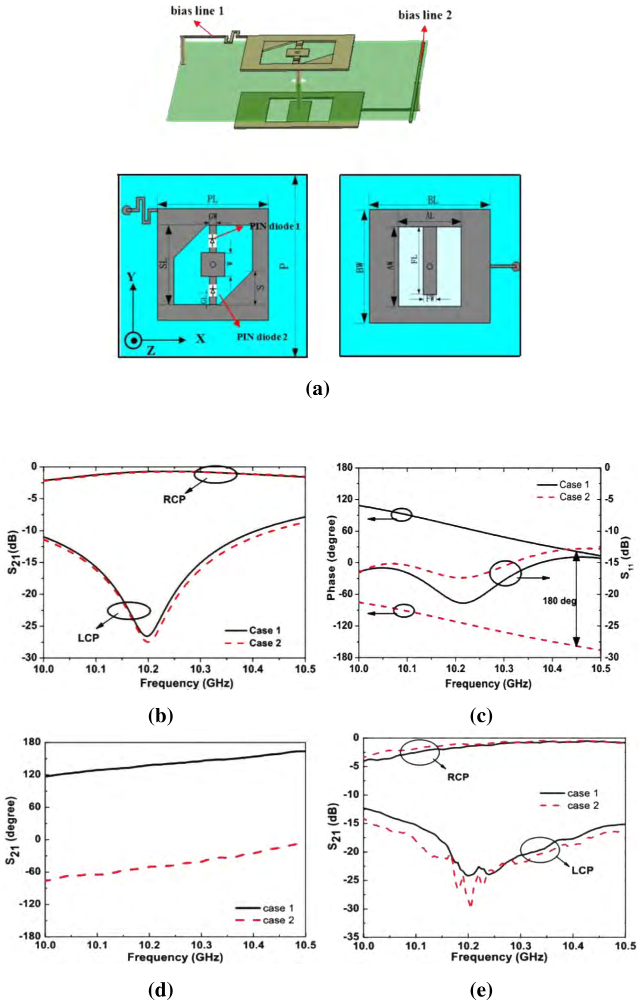

FIGURE 20. (a) Transmitarray unit-cell design loaded with p-i-n diodes; S_{21} amplitude and phase response for: (b,c) simulated and (d,e) experimental results, respectively (images extracted from the work presented in [77]).

with two p-i-n diodes inserted along the x and y directions in order to control the polarization of the outgoing wave. According to simulations, the insertion loss of the unit-cell varies between 1.5 and 5 dB at frequencies around 5.4 GHz, and a cross-polarization ratio higher than 25 dB is obtained. The 8×8 transmitarray prototype is illustrated in Figs 19b and 19c. Experimental results demonstrate that this transmitarray is capable of achieving $\pm 60°$ in both azimuth and elevation planes, having a difference of 3.8 dB between the gain of the broadside beam and at the scan angle of 60°. Experimental results also show that this transmitarray is capable of producing an outgoing wave with circular polarization by controlling each of the p-i-n diodes independently.

In [77] yet another transmitarray with polarization control capabilities is presented by the same authors of [76], based on the unit-cell of Fig. 20. The authors have suggested two designs of unit-cells for 1-bit phase resolution transmitarray, to operate around 10 GHz. The most complete design presented by the authors consists of two-layer metallic patterns connected by a metallized via-hole as depicted in Fig. 20a.

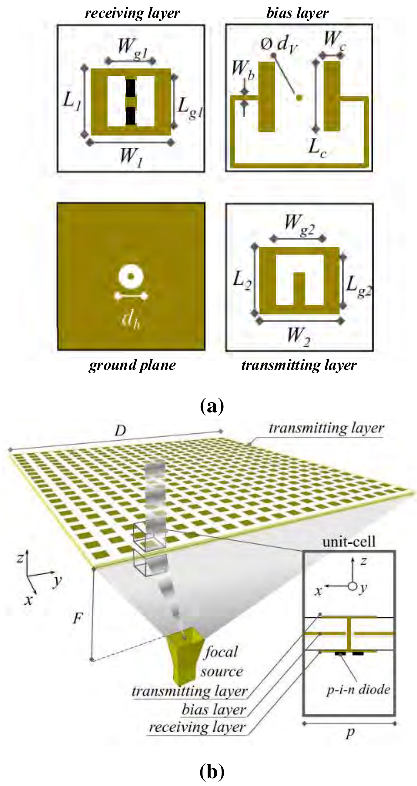

FIGURE 21. Snapshot of (a) the active unit-cell and (b) transmitarray for beamsteering and polarization control (images extracted from the work presented in [79]).

A U-slot rectangular patch is used in one side of the structure to receive the incident wave. On the other side, a square ring patch with two triangular corners and loaded with 2 p-i-n diodes is utilized to produce circular polarization. The p-i-n diodes were used to dynamically select between LHCP and RHCP. The unit-cell operates under two cases: case 1 - p-i-n diode 1 is switched on while 2 is off; case 2 - p-i-n diode 1 is switched off while 2 is on. Simulated results (Fig. 20b, Fig. 20c) on the unit-cell were further validated on a 8×8 transmitarray prototype against experimental results (Fig. 20d, Fig. 20e). While in case 1, the transmitarray converts a vertically polarized incident wave to RHCP, in case 2 the transmission phase of the outgoing wave is also shifted by 180°. Based on the previous unit-cell design [77], the same research group have introduced and characterized in [78], a transmitarray with both reconfigurable polarization control and beamsteering capabilities. Besides of controlling the polarization of the re-transmitted EM wave, the proposed transmitarray also has the capability of realizing beamsteering in a range of $\pm 45°$ in both elevation an azimuth planes at 4.8 GHz, exhibiting however insertion losses of 5.6 dB over a small bandwidth of 100 MHz, obtained experimentally on a manufactured prototype.

Similarly in [79], it has been presented a 20×20 element fully reconfigurable transmitarray based on a 1-bit linear polarization unit-cell model operating in the Ka-band (27-GHz). A snapshot of both unit-cells and the reconfigurable transmitarray are depicted in Fig. 21. The unit-cell is

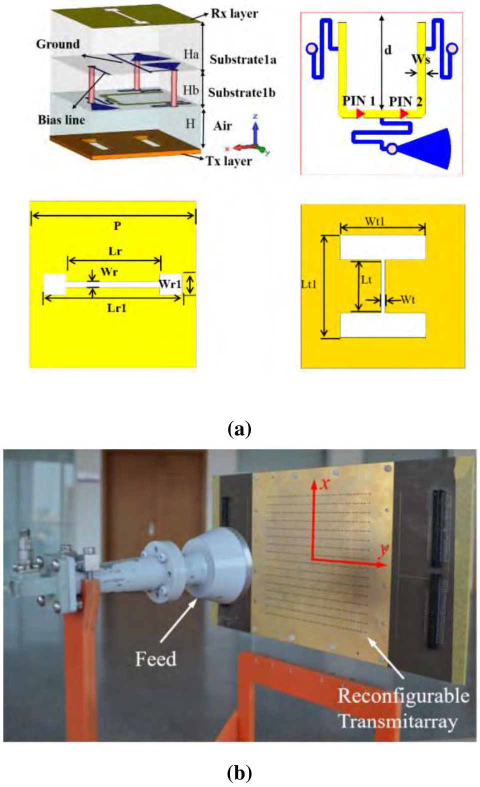

FIGURE 22. (a) Geometry of the transmitarray element and (b) reconfigurable transmitarray prototype with 16 × 16 elements (images extracted from the work presented in [80]).

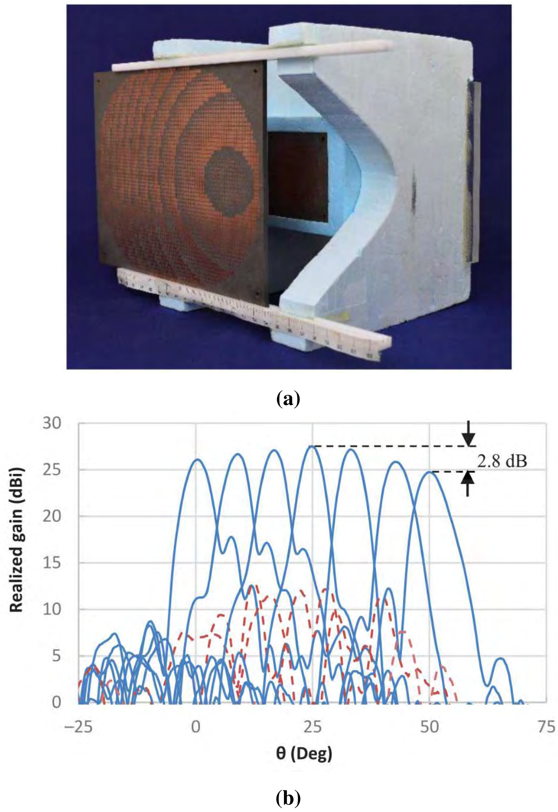

FIGURE 23. (a) Antenna prototype and (b) measured realized gain for several beamsteering angles between 0° and 50° (images extracted from the work presented in [81]).

formed in a multi-layer design with a central ground plane (Fig. 21a) loaded with p-i-n diodes to obtain a wide-band constant phase shift between the two phase states. Circular polarization is achieved by using the sequential rotation technique previously described, while p-i-n diodes enable LHCP / RHCP polarization switching. However, due to the control of the phase shift by switching on and off the p-i-n diodes, the control of the direction of the out-coming wave is also possible with reported steering ranges of ±60° in azimuth and elevation planes.

Finally, in [80] a 1-bit reconfigurable transmitarray that allows control of polarization as well as antenna beamsteering is presented. The unit-cell of the transmitarray is comprised of two H-shaped slots (Fig. 22a) that behave as receiving and transmitting coupled microstrip patches. The fact that they are orthogonality disposed relative to each other, it allows X to Y polarization transformation (of the incident EM wave). In between the transmitter and receiver slot patches, a feeding network that includes 2 p-i-n diodes is responsible to control the phase difference of the arrangement. When the p-i-n diode 1 is OFF and p-i-n diode 2 is ON (Fig. 22a), a total phase shift of 180° is achieved against 0° phase shift for the opposite case. The proposed unit-cell operates at a center frequency of 12.5 GHz and it has an overall dimension of 8×8 mm^2 ($\lambda/3 \times \lambda/3$). According to simulation on the unit-cell, the -10 dB S_{11} bandwidth is of 300 MHz for both working cases, with maximum of 0.86 dB of insertion losses (for the case where D1=OFF/D2=ON). The isolation between co- and cross-polarizations is 16.5 dB for the center frequency.

Subsequent to the unit-cell characterization, a 16 × 16 transmitarray prototype has been fabricated and measured. It is composed of 256 individual cells leading to a total of 512 p-i-n diodes to achieve both phase and angular reconfigurability. A *x-polarized* horn feed is used to illuminate the transmitarray as shown in Fig. 22b. With the presented setup, a total of ±50° beamsteering is obtained for both elevation and azimuth planes.

It should be noted that some authors consider that the transmitarray are placed at a distance far away from the radiation source aperture (focal distance), whereas others are considered at the vicinity of the antenna source aperture. The ones that are placed at the right focal distance typically exhibit wide beamsteering ranges, since the placement at the focal distance leads to better spillover and illumination efficiencies.

In fact, this is well reported in [81] where the authors have developed a flat lens exhibiting circular polarization and wide beamsteering angular ranges (Fig. 23). In particular, the focal seems to play distance play an important role in radiation performance, since larger distances tend to reduce aberration and consequently lower beam distortions and improve side-lobe levels. To this end, the authors in [81] have proposed a new feeding technique by implementing a virtual focus using a dual-lens configuration, in order to

TABLE 1. Summary table of references for polarization control (Pol.) and beamsteering (BS) transmitarrays.

Ref.	Feature	Mode†	UC type	UC size	Control mechanism	Freq. band	Bandwidth	Loss	BS Range
[37]	BS	A	microstrip patch	n/a	varactor	12 GHz	700 MHz	3 dB	$+9^\circ (Az\ only)$
[38], [39]		A	microstrip patch	$0.55\lambda \times 0.55\lambda$	varactor	5.7 GHz	n/a	4.8dB	$\pm 25^{\circ\star} (Az\ or\ El)$
[40]		A	coupled feed patch	$0.55\lambda \times 0.55\lambda$*	varactor	5 GHz*	500 MHz*	3.6 dB*	n/a
[41]		A	coupled feed patch	$0.55\lambda \times 0.55\lambda$	varactor	5 GHz	500 MHz	2.2 dB	$\pm 50^{\circ\star} (Az\ and\ El)$
[42]–[44]		A	microstrip patch	$0.5\lambda \times 0.5\lambda$	p-i-n (and MEMS)	10 GHz	1.5 GHz	3 dB	$\pm 70^\circ (Az)\ and\ \pm 40^\circ (El)$
[45]		A	O-slot rectangular patch	$\lambda/2 \times \lambda/2$	p-i-n	29 GHz	n/a	n/a	$\pm 40^{\circ\star} (Az\ only)$
[46]		A	microstrip patch	n/a	varactor diodes	24.6 GHz	1 GHz	17 dB	$\pm 50^\circ (Az\ and\ El)$
[14]		A	metamaterials	n/a	liquid crystal	27.5 GHz	n/a	5 dB	$\pm 5^\circ (Az\ only)$
[47]		A	metamaterials	$0.17\lambda \times 0.17\lambda$	varactor	1.7 GHz	n/a	4 dB	$\pm 30^{\circ\star} (Az\ only)$
[48]		A	metamaterials	$0.61\lambda \times 0.61\lambda$	varactor	4.7 GHz	250 MHz	n/a	$\pm 30^{\circ\star} (Az\ only)$
[49]–[51]		A	freq. selective surface	$0.5\lambda \times 0.5\lambda$*	varactor	4 GHz*	400 MHz*	3 dB*	n/a
[52]		A	freq. selective surface	$0.58\lambda \times 0.58\lambda$	varactor	5.3 GHz	180 MHz	6.5 dB	$\pm 30^{\circ\star} (Az\ or\ El)$
[53]		A	freq. selective surface	$\lambda/25 \times \lambda/25$	tunable ferroelectric film	12 GHz	n/a	2.9 dB	$\pm 10^\circ (Az\ only)$
[54]		P	freq. selective surface	$0.17\lambda \times 0.17\lambda$	discrete capacitors	5.35 GHz	110 MHz	2.8 dB	$\pm 25^\circ (Az\ and\ El)$
[55]		A	freq. selective surface	$0.17\lambda \times 0.17\lambda$	varactor	5.2 GHz	70 MHz	4.3 dB	$\pm 28^\circ (Az)\ and\ \pm 26^\circ (El)$
[56]		A	freq. selective surface	$0.54\lambda \times 0.54\lambda$	p-i-n	11.5 GHz	n/a	n/a	$\pm 40^\circ (Az\ and\ El)$
[62], [63]	Pol	P	microstrip patch	$0.5\lambda \times 0.5\lambda$*	cell rotation	60 GHz*	5.6 GHz*	0.46 dB*	n/a
[64]		P	microstrip patch	$0.5\lambda \times 0.5\lambda$	cell rotation	30 GHz	6.5 GHz	n/a	n/a
[65]		P	multi-layer PCB	$0.28\lambda \times 0.28\lambda$	cascading surfaces	77 GHz	13 GHz	n/a	n/a
[66]		P	cascaded rectangle ring slot	$0.6\lambda \times 0.6\lambda$	feeding source rotation	6 GHz	1.8 GHz	n/a	n/a
[76]	Hybrid (BS & Pol)	A	square patch	$0.482\lambda \times 0.482\lambda$	varactor (and p-i-n)	5.4 GHz	450 MHz	3.8 dB	$\pm 60^\circ (Az\ and\ El)$
[77]		A	U-slot patch	$0.47\lambda \times 0.47\lambda$	p-i-n	10 GHz	320 MHz	1.4 dB	n/a
[78]		A	U-slot coupled feed patch	$0.488\lambda \times 0.488\lambda$	p-i-n	4.8 GHz	100 MHz	5.6 dB	$\pm 45^\circ (Az\ and\ El)$
[79]		A	rectangle ring slot	$0.46\lambda \times 0.46\lambda$	p-i-n	27 GHz	4.2 GHz	3 dB	$\pm 60^\circ (Az\ and\ El)$
[80]		A	U-shaped microstrip line	$\lambda/3 \times \lambda/3$	p-i-n	12.5 GHz	300 MHz	5 dB	$\pm 50^\circ (Az\ and\ El)$
[81]		P	dual layer microstrip patch	$\lambda/3 \times \lambda/3$	n/a	30 GHz	2 GHz	n/a	$\pm 50^\circ (El)$

† modes for unit-cells: P - passive, A - active (reconfigurable);
* considering the best case of 2 proposed designs;
$\star$ steering range with SLL<12dB;
n/a - not available.

reduce the overall antenna height. Remarkably, beamsteering angles up to ±50°, at Ka-band (30 GHz) with an antenna height estimated to be reduced by 20%, due to the virtual focus, has been achieved. In fact, this is different technique to those previously presented, in which a lens-like phase pattern, by means of microstrip patches, is used for beamsteering.

The closer the feed, the higher the oblique incident angle, which in turn affects negatively the illumination efficiency and thus overall steering ranges. However, the transmitarray placed right next to antenna aperture also showed to processing results with the advantage of reducing the overall size of the apparatus.

The references presented in this review of the literature are summarized in Table 1, listed by their main feature (polarization control and beamsteering), mode of operation (P - passive, A - active), unit-cell (UC) design format and size, reconfigurability control mechanism, frequency of operation, bandwidth, insertion losses and beamsteering angular ranges with respective steering planes, when applicable.

IV. CONCLUSIONS

This paper presents an extensive literature review addressing antenna beamsteering by using transmitarray. A fundamental overview on the concept of 1D and 2D beamsteering using a transmitarray is presented. With this, it was verified that to perform beamsteering with a transmitarray, the phase in each transmitarray element must be varied, progressively and equally, throughout the entire array much like a phased antenna array. Subsequently, a dedicated literature review is outlined starting with transmitarray developed for antenna beamsteering, wavefront polarization control, and transmitarray that combine both features simultaneity. Particular emphasis is given to active/reconfigurable transmitarray, *i.e.* devices with the capability of having its characteristics electronically controlled, either by employing active mechanisms as p-i-n diodes, varactor diodes or MEMS switches. Several examples among the literature have been presented and compared, followed by a critical review. Information about unit-cell main characteristics are disseminated including, design layout, *e.g.* if based on FSS, MM or microstrip patch antennas. Finally, all this information is summarized in terms of useful technical data extracted from the literature such as, frequency of operation, bandwidth, unit/cell dimensions, insertion loss and maximum steering ranges. This review paper demonstrates that transmitarray antennas can be seen as a feasible alternative to the most traditional techniques of beamsteering, overcoming some of its limitations, e.g. it withdraws the requirements of complex beamsteering networks of phased antenna arrays. Since transmitarray are mostly employing using PCB techniques, they will significantly reduce weight, power consumption and the dimensions of assemblies, making them very attractive for inclusion in a large number of applications. Future work may address study of new methods to increase beamsteering ranges, e.g. using conformal transmitarray, while enabling finer angular resolution, polarization control (for polarimetric applications) and beam (de)focusing. New reconfigurable unit-cell designs is of paramount importance to overcome existing limitations, as outlined in this paper, in terms of bandwidth, insertion losses and phase ranges. Of utterly importance is also the extension of the supporting technology from PCB to system on chip (SoC), being one forward leap from vertical (stacked) integration of layers to save space and improve on the massive integration of active components, whilst exploring new designs based on novel electronic biasing (tunable) metamaterials. Finally, beamsteering based on transmitarray is currently well perceived as one of the most important key enabling technologies to achieve multi-gigabit/s peak data rates in mobile radio channels. Emerging 5G systems and beyond may encompass fundamentally new transmitarray designs targeting micro- and millimeter-wave frequencies, small form factors and light-weight solutions, enabling the development of new agile beamsteering and user tracking algorithms.

REFERENCES

[1] C. A. Balanis, *Antenna Theory and Design*, vol. 72, 3rd ed. Hoboken, NJ, USA: Wiley, 2005.

[2] R. J. Mailloux, *Phased Array Antenna Handbook*. Norwood, MA, USA: Artech House, 2005.

[3] A. K. Bhattacharyya, *Phased Array Antennas: Floquet Analysis, Synthesis, Bfns and Active Array Systems* (Wiley Series in Microwave and Optical Engineering). Hoboken, NJ, USA: Wiley, 2006.

[4] D. T. McGrath, "Planar three-dimensional constrained lenses," *IEEE Trans. Antennas Propag.*, vol. AP-34, no. 1, pp. 46–50, Jan. 1986.

[5] J. Y. Lau, "Reconfigurable transmitarray antennas," Ph.D. dissertation, Dept. Elect. Comput. Eng., Univ. Toronto, Toronto, ON, Canada, 2012.

[6] L. D. Palma, "Reconfigurable transmitarray antennas at millimeter-wave frequencies," Ph.D. dissertation, École Doctorale Math., Télécommun., Inform., Signal, Syst., Électron., Univ. Rennes, Rennes, France, 2015.

[7] S. V. Hum and J. Perruisseau-Carrier, "Reconfigurable reflectarrays and array lenses for dynamic antenna beam control: A review," *IEEE Trans. Antennas Propag.*, vol. 62, no. 1, pp. 183–198, Jan. 2014.

[8] F. Capolino, *Applications of Metamaterials*. Boca Raton, FL, USA: CRC Press, 2009.

[9] C. Balanis, *Advanced Engineering Electromagnetics* (Coursesmart). Hoboken, NJ, USA: Wiley, 2012.

[10] J. C. Vardaxoglou, *Frequency Selective Surfaces—Analysis & Design*. Taunton, U.K.: Research Studies Press, 1997.

[11] B. A. Munk, *Frequency Selective Surfaces: Theory and Design*. Hoboken, NJ, USA: Wiley, 2005.

[12] K. Sarabandi and N. Behdad, "A frequency selective surface with miniaturized elements," *IEEE Trans. Antennas Propag.*, vol. 55, no. 5, pp. 1239–1245, May 2007.

[13] D. Ferreira, R. Caldeirinha, I. Cuiñas, and T. Fernandes, "Square loop and slot frequency selective surfaces study for equivalent circuit model optimization," *IEEE Trans. Antennas Propag.*, vol. 63, no. 9, pp. 3947–3955, Sep. 2015.

[14] M. Maasch, M. Roig, C. Damm, and R. Jakoby, "Voltage-tunable artificial gradient-index lens based on a liquid crystal loaded fishnet metamaterial," *IEEE Antennas Wireless Propag. Lett.*, vol. 13, pp. 1581–1584, 2014.

[15] Y. Huang, L. S. Wu, M. Tang, and J. Mao, "Design of a beam reconfigurable THz antenna with graphene-based switchable high-impedance surface," *IEEE Trans. Nanotechnol.*, vol. 11, no. 4, pp. 836–842, Jul. 2012.

[16] E. Carrasco, M. Tamagnone, and J. Perruisseau-Carrier, "Tunable graphene-based reflectarray element for reconfigurable beams," in *Proc. 7th Eur. Conf. Antennas Propag. (EuCAP)*, Apr. 2013, pp. 1779–1782.

[17] H. A. Malhat, S. H. Zainud-Deen, and S. M. Gaber, "Circularly polarized graphene based transmitarray for terahertz applications," in *Proc. 31st Gen. Assem. Sci. Symp. (URSI GASS)*, Aug. 2014, pp. 1–4.

[18] W. M. Hassan, S. H. Zainud-Deen, and H. A. Malhat, "Compact multi-function single/dual-beam graphene lens antenna for terahertz applications," in *Proc. 33rd Nat. Radio Sci. Conf. (NRSC)*, Feb. 2016, pp. 41–48.

[19] W. M. Hassan, "Multilayer graphene-only transmitarray antenna (MGOT) for terahertz applications," in *Proc. 34th Nat. Radio Sci. Conf. (NRSC)*, Mar. 2017, pp. 43–48.

[20] W. Yao, L. Tang, J. Wang, C. Ji, X. Wei, and Y. Jiang, "Spectrally and spatially tunable terahertz metasurface lens based on graphene surface plasmons," *IEEE Photon. J.*, vol. 10, no. 4, pp. 1–8, Aug. 2018.

[21] A. Moessinger, R. Marin, S. Mueller, J. Freese, and R. Jakoby, "Electronically reconfigurable reflectarrays with nematic liquid crystals," *Electron. Lett.*, vol. 42, no. 16, pp. 899–900, Aug. 2006.

[22] G. Perez-Palomino, J. A. Encinar, M. Barba, and E. Carrasco, "Design and evaluation of multi-resonant unit cells based on liquid crystals for reconfigurable reflectarrays," *IET Microw., Antennas Propag.*, vol. 6, no. 3, pp. 348–354, Feb. 21, 2012.

[23] S. Bildik, S. Dieter, C. Fritzsch, W. Menzel, and R. Jakoby, "Reconfigurable folded reflectarray antenna based upon liquid crystal technology," *IEEE Trans. Antennas Propag.*, vol. 63, no. 1, pp. 122–132, Jan. 2015.

[24] G. Perez-Palomino, M. Barba, J. A. Encinar, R. Cahill, R. Dickie, P. Baine, and M. Bain, "Design and demonstration of an electronically scanned reflectarray antenna at 100 GHz using multiresonant cells based on liquid crystals," *IEEE Trans. Antennas Propag.*, vol. 63, no. 8, pp. 3722–3727, Aug. 2015.

[25] Y. Zhao, C. Huang, A.-Y. Qing, and X. Luo, "A frequency and pattern reconfigurable antenna array based on liquid crystal technology," *IEEE Photon. J.*, vol. 9, no. 3, pp. 1–7, Jun. 2017.

[26] B.-J. Che, T. Jin, D. Erni, F.-Y. Meng, Y.-L. Lyu, and Q. Wu, "Electrically controllable composite right/left-handed leaky-wave antenna using liquid crystals in PCB technology," *IEEE Trans. Compon., Packag., Manuf. Technol.*, vol. 7, no. 8, pp. 1331–1342, Aug. 2017.

[27] S. F. Jilani, M. O. Munoz, Q. H. Abbasi, and A. Alomainy, "Millimeter-wave liquid crystal polymer based conformal antenna array for 5G applications," *IEEE Antennas Wireless Propag. Lett.*, vol. 18, no. 1, pp. 84–88, Jan. 2019.

[28] S. H. Lee, M. Choi, T.-T. Kim, S. Lee, M. Liu, X. Yin, H. K. Choi, S. S. Lee, C.-G. Choi, S.-Y. Choi, X. Zhang, and B. Min, "Switching terahertz waves with gate-controlled active graphene metamaterials," *Nature Mater.*, vol. 11, pp. 936–941, Sep. 2012. doi: 10.1038/nmat3433.

[29] C. N. Álvarez, R. Cheung, and J. S. Thompson, "Performance analysis of hybrid metal–graphene frequency reconfigurable antennas in the microwave regime," *IEEE Trans. Antennas Propag.*, vol. 65, no. 4, pp. 1558–1569, Apr. 2017.

[30] J. Shaker, M. R. Chaharmir, and J. Ethier, *Reflectarray Antennas: Analysis, Design, Fabrication, and Measurement*, vol. 1. Norwood, MA, USA: Artech House, 2013.

[31] J. Huang and J. A. Encinar, *Reflectarray Antennas*, vol. 9. Hoboken, NJ, USA: Wiley, 2007.

[32] D. M. Pozar, S. D. Targonski, and H. D. Syrigos, "Design of millimeter wave microstrip reflectarrays," *IEEE Trans. Antennas Propag.*, vol. 45, no. 2, pp. 287–296, Feb. 1997.

[33] D. Sievenpiper, J. Schaffner, R. Loo, G. Tangonan, S. Ontiveros, and R. Harold, "A tunable impedance surface performing as a reconfigurable beam steering reflector," *IEEE Trans. Antennas Propag.*, vol. 50, no. 3, pp. 384–390, Mar. 2002.

[34] D. Sievenpiper and J. Schaffner, "Beam steering microwave reflector based on electrically tunable impedance surface," *Electron. Lett.*, vol. 38, no. 21, pp. 1237–1238, Oct. 2002.

[35] E. Carrasco, M. Barba, B. Reig, C. Dieppedale, and J. A. Encinar, "Characterization of a reflectarray gathered element with electronic control using ohmic RF MEMS and patches aperture-coupled to a delay line," *IEEE Trans. Antennas Propag.*, vol. 60, no. 9, pp. 4190–4201, Sep. 2012.

[36] E. Carrasco, M. Barba, and J. A. Encinar, "X-band reflectarray antenna with switching-beam using PIN diodes and gathered elements," *IEEE Trans. Antennas Propag.*, vol. 60, no. 12, pp. 5700–5708, Dec. 2012.

[37] P. Padilla, A. Muñoz-Acevedo, M. Sierra-Castaner, and M. Sierra-Perez, "Electronically reconfigurable transmitarray at Ku band for microwave applications," *IEEE Trans. Antennas Propag.*, vol. 58, no. 8, pp. 2571–2579, Aug. 2010.

[38] J. Y. Lau and S. V. Hum, "Analysis and characterization of a multipole reconfigurable transmitarray element," *IEEE Trans. Antennas Propag.*, vol. 59, no. 1, pp. 70–79, Jan. 2011.

[39] J. Y. Lau and S. V. Hum, "A planar reconfigurable aperture with lens and reflectarray modes of operation," *IEEE Trans. Microw. Theory Techn.*, vol. 58, no. 12, pp. 3547–3555, Dec. 2010.

[40] J. Y. Lau and S. V. Hum, "A wideband reconfigurable transmitarray element," *IEEE Trans. Antennas Propag.*, vol. 60, no. 3, pp. 1303–1311, Mar. 2012.

[41] J. Y. Lau and S. V. Hum, "Reconfigurable transmitarray design approaches for beamforming applications," *IEEE Trans. Antennas Propag.*, vol. 60, no. 12, pp. 5679–5689, Dec. 2012.

[42] A. Clemente, L. Dussopt, R. Sauleau, P. Potier, and P. Pouliguen, "1-bit reconfigurable unit cell based on PIN diodes for transmit-array applications in X-band," *IEEE Trans. Antennas Propag.*, vol. 60, no. 5, pp. 2260–2269, May 2012.

[43] A. Clemente, L. Dussopt, B. Reig, R. Sauleau, P. Potier, and P. Pouliguen, "Reconfigurable unit-cells for beam-scanning transmitarrays in X band," in *Proc. 7th Eur. Conf. Antennas Propag. (EuCAP)*, Apr. 2013, pp. 1783–1787.

[44] A. Clemente, L. Dussopt, R. Sauleau, P. Potier, and P. Pouliguen, "Wideband 400-element electronically reconfigurable transmitarray in X band," *IEEE Trans. Antennas Propag.*, vol. 61, no. 10, pp. 5017–5027, Oct. 2013.
[45] F. Diaby, A. Clemente, L. Di Palma, L. Dussopt, K. Pham, E. Fourn, and R. Sauleau, "Design of a 2-bit unit-cell for electronically reconfigurable transmitarrays at ka-band," in *Proc. IEEE 47th Eur. Microw. Conf. (EuMC)*, Oct. 2017, pp. 1321–1324.
[46] M. Frank, F. Lurz, R. Weigel, and A. Koelpin, "Electronically reconfigurable 6×6 element transmitarray at K-band based on unit cells with continuous phase range," *IEEE Antennas Wireless Propag. Lett.*, vol. 18, no. 4, pp. 796–800, Apr. 2019.
[47] Y. Sun, Z. Li, W. Zhu, Z. Ji, and Q. Wang, "New steerable antenna with controllable metamaterial," in *Proc. 9th Eur. Radar Conf. (EuMC)*, Oct./Nov. 2012, pp. 610–613.
[48] T. Jiang, Z. Wang, D. Li, J. Pan, B. Zhang, J. Huangfu, Y. Salamin, C. Li, and L. Ran, "Low-DC voltage-controlled steering-antenna radome utilizing tunable active metamaterial," *IEEE Trans. Microw. Theory Techn.*, vol. 60, no. 1, pp. 170–178, Jan. 2012.
[49] I. Russo, D. Gaetano, L. Boccia, G. Amendola, and G. Di Massa, "Investigation on the transmission beam-steering capabilities of tunable impedance surfaces," in *Proc. Eur. Microw. Conf. (EuMC)*, Sep./Oct. 2009, pp. 1033–1036.
[50] I. Russo, L. Boccia, G. Amendola, and G. Di Massa, "Tunable pass-band FSS for beam steering applications," in *Proc. 4th Eur. Conf. Antennas Propag. (EuCAP)*, Apr. 2010, pp. 1–4.
[51] L. Boccia, I. Russo, G. Amendola, and G. D. Massa, "Multilayer antenna-filter antenna for beam-steering transmit-array applications," *IEEE Trans. Microw. Theory Techn.*, vol. 60, no. 7, pp. 2287–2300, Jul. 2012.
[52] W. Pan, C. Huang, P. Chen, M. Pu, X. Ma, and X. Luo, "A beam steering horn antenna using active frequency selective surface," *IEEE Trans. Antennas Propag.*, vol. 61, no. 12, pp. 6218–6223, Dec. 2013.
[53] M. Sazegar, Y. Zheng, C. Kohler, H. Maune, M. Nikfalazar, J. R. Binder, and R. Jakoby, "Beam steering transmitarray using tunable frequency selective surface with integrated ferroelectric varactors," *IEEE Trans. Antennas Propag.*, vol. 60, no. 12, pp. 5690–5699, Dec. 2012.
[54] J. R. Reis, N. Copner, A. Hammoudeh, Z. M.-E. Al-Daher, R. F. S. Caldeirinha, T. R. Fernandes, and R. Gomes, "FSS-inspired transmitarray for two-dimensional antenna beamsteering," *IEEE Trans. Antennas Propag.*, vol. 64, no. 6, pp. 2197–2206, Jun. 2016.
[55] J. R. Reis, R. F. S. Caldeirinha, A. Hammoudeh, and N. Copner, "Electronically reconfigurable FSS-inspired transmitarray for 2-D beamsteering," *IEEE Trans. Antennas Propag.*, vol. 65, no. 9, pp. 4880–4885, Sep. 2017.
[56] B. D. Nguyen and C. Pichot, "Unit-cell loaded with PIN diodes for 1-bit linearly polarized reconfigurable transmitarrays," *IEEE Antennas Wireless Propag. Lett.*, vol. 18, no. 1, pp. 98–102, Jan. 2019.
[57] G. F. Masters and S. F. Gregson, "Coordinate system plotting for antenna measurements," in *Proc. AMTA Symp.*, 2007, pp. 1–10.
[58] C. G. M. Ryan, M. R. Chaharmir, J. Shaker, J. R. Bray, Y. M. M. Antar, and A. Ittipiboon, "A wideband transmitarray using dual-resonant double square rings," *IEEE Trans. Antennas Propag.*, vol. 58, no. 5, pp. 1486–1493, May 2010.
[59] A. Edalati and T. A. Denidni, "Beam-switching antenna based on active frequency selective surfaces," in *Proc. IEEE Int. Symp. Antennas Propag. (APSURSI)*, Jul. 2011, pp. 2254–2257.
[60] H. Zhou, S. Qu, B. Lin, J. Wang, H. Ma, Z. Xu, W. Peng, and P. Bai, "Filter-antenna consisting of conical FSS radome and monopole antenna," *IEEE Trans. Antennas Propag.*, vol. 60, no. 6, pp. 3040–3045, Jun. 2012.
[61] M. Niroo-Jazi and T. A. Denidni, "Electronically sweeping-beam antenna using a new cylindrical frequency-selective surface," *IEEE Trans. Antennas Propag.*, vol. 61, no. 2, pp. 666–676, Feb. 2013.
[62] H. Kaouach, L. Dussopt, J. Lantéri, T. Koleck, and R. Sauleau, "Circularly-polarized discrete lens antennas in the 60-GHz band," in *Proc. ICECom*, Sep. 2010, pp. 1–4.
[63] L. Dussopt, H. Kaouach, J. Lanteri, and R. Sauleau, "Circularly-polarized discrete lens antennas in the 60-GHz band," *Radio Eng.*, vol. 20, pp. 733–738, Dec. 2011.
[64] L. Di Palma, A. Clemente, L. Dussopt, R. Sauleau, P. Potier, and P. Pouliguen, "Circularly polarized transmitarray with sequential rotation in Ka-band," *IEEE Trans. Antennas Propag.*, vol. 63, no. 11, pp. 5118–5124, Nov. 2015.
[65] C. Pfeiffer and A. Grbic, "Millimeter-wave transmitarrays for wavefront and polarization control," *IEEE Trans. Microw. Theory Techn.*, vol. 61, no. 12, pp. 4407–4417, Dec. 2013.
[66] X. Zhong, L. Chen, Y. Shi, and X. Shi, "Design of multiple-polarization transmitarray antenna using rectangle ring slot elements," *IEEE Antennas Wireless Propag. Lett.*, vol. 15, pp. 1803–1806, 2016.
[67] P. Naseri, S. A. Matos, J. R. Costa, and C. A. Fernandes, "Phase-delay versus phase-rotation cells for circular polarization transmit arrays—Application to satellite Ka-band beam steering," *IEEE Trans. Antennas Propag.*, vol. 66, no. 3, pp. 1236–1247, Mar. 2018.
[68] S. Hollung, A. E. Cox, and Z. B. Popovic, "A bi-directional quasi-optical lens amplifier," *IEEE Trans. Microw. Theory Techn.*, vol. 45, no. 12, pp. 2352–2357, Dec. 1997.
[69] E. W. Bryerton, M. D. Weiss, and Z. Popovic, "A 10-GHz high-efficiency lens amplifier array," in *IEEE MTT-S Int. Microw. Symp. Dig.*, vol. 3, Jun. 1998, pp. 1461–1464.
[70] S. C. Ortiz, T. Ivanov, and A. Mortazawi, "A CPW-fed microstrip patch quasi-optical amplifier array," *IEEE Trans. Microw. Theory Techn.*, vol. 48, no. 2, pp. 276–280, Feb. 2000.
[71] H. J. Song and M. E. Bialkowski, "Transmit array of transistor amplifiers illuminated by a patch array in the reactive near-field region," *IEEE Trans. Microw. Theory Techn.*, vol. 49, no. 3, pp. 470–475, Mar. 2001.
[72] S. C. Ortiz, J. Hubert, L. Mirth, E. Schlecht, and A. Mortazawi, "A high-power Ka-band quasi-optical amplifier array," *IEEE Trans. Microw. Theory Techn.*, vol. 50, no. 2, pp. 487–494, Feb. 2002.
[73] W. Pan, C. Huang, X. Ma, and X. Luo, "An amplifying tunable transmitarray element," *IEEE Antennas Wireless Propag. Lett.*, vol. 13, pp. 702–705, 2014.
[74] N. Landsberg and E. Socher, "Multi-level ASK spatial modulators employing a 100 GHz lens-array antenna and 65 nm CMOS," in *Proc. 46th Eur. Microw. Conf. (EuMC)*, Oct. 2016, pp. 429–432.
[75] N. Landsberg and E. Socher, "Design and measurements of 100 GHz reflectarray and transmitarray active antenna cells," *IEEE Trans. Antennas Propag.*, vol. 65, no. 12, pp. 6986–6997, Dec. 2017.
[76] C. Huang, W. Pan, X. Ma, B. Zhao, J. Cui, and X. Luo, "Using reconfigurable transmitarray to achieve beam-steering and polarization manipulation applications," *IEEE Trans. Antennas Propag.*, vol. 63, no. 11, pp. 4801–4810, Nov. 2015.
[77] C. Huang, W. Pan, X. Ma, and X. Luo, "1-bit reconfigurable circularly polarized transmitarray in X-band," *IEEE Antennas Wireless Propag. Lett.*, vol. 15, pp. 448–451, Jul. 2015.
[78] C. Huang, W. Pan, and X. Luo, "Low-loss circularly polarized transmitarray for beam steering application," *IEEE Trans. Antennas Propag.*, vol. 64, no. 10, pp. 4471–4476, Oct. 2016.
[79] L. D. Palma, A. Clemente, L. Dussopt, R. Sauleau, P. Potier, and P. Pouliguen, "Circularly-polarized reconfigurable transmitarray in Ka-band with beam scanning and polarization switching capabilities," *IEEE Trans. Antennas Propag.*, vol. 65, no. 2, pp. 529–540, Feb. 2017.
[80] M. Wang, S. Xu, F. Yang, and M. Li, "Design and measurement of a 1-bit reconfigurable transmitarray with subwavelength H-shaped coupling slot elements," *IEEE Trans. Antennas Propag.*, vol. 67, no. 5, pp. 3500–3504, May 2019.
[81] E. B. Lima, S. A. Matos, J. R. Costa, C. A. Fernandes, and N. J. G. Fonseca, "Circular polarization wide-angle beam steering at Ka-band by in-plane translation of a plate lens antenna," *IEEE Trans. Antennas Propag.*, vol. 63, no. 12, pp. 5443–5455, Dec. 2015.

JOAO R. REIS was born in Lisbon, Portugal, in 1987. He received the undergraduate degree in Electrical Engineering, Electronics & Telecommunications, from the School of Technology and Management (ESTG) of the Polytechnic Institute of Leiria (IPL), Portugal, in 2010. In 2018, he was awarded a Ph.D in Electrical Engineering, specialization in antennas and propagation, by the University of South Wales, Treforest, United Kingdom, for his research work on the topic: "Novel antenna beamsteering for wireless applications". Currently, he is a full-time researcher at Instituto de Telecomunicações, Portugal–research group of Antennas & Propagation-Leiria (A&P-Lr), working in project RADAVANT (FEDER/POCENTRO/SI-IDT, 03/SI/2017–Project no. 033907). He is also an invited lecturer at Polytechnic Institute of Leiria, Leiria, Portugal. His current research interests include antennas and radio wave propagation, beamsteering antenna systems and RADAR, frequency selective surfaces and metamaterials.

MARIO VALA was born in Leiria, Portugal, in 1996. He received the bachelor's degree in electrical and computer engineering and electronics and computers from the School of Technology and Management (ESTG), Polytechnic Institute of Leiria (IPL), Portugal, in 2017. He is currently pursuing the M.Sc. degree with the School of Technology and Management (ESTG), Polytechnic Institute of Leiria (IPL), Portugal. His M.Sc. thesis was entitled Transmitarray for Antenna Beamsteering at 28 GHz. He is currently a Researcher with the Antennas & Propagation (A&P-Lr) Research Group, Instituto de Telecomunicações, Leiria.

RAFAEL F. S. CALDEIRINHA was born in Leiria, Portugal, in 1974. He received the B.Eng. degree (Hons) in electronic and communication engineering and the Ph.D. degree in radiowave propagation from the University of Glamorgan, U.K., in 1997 and 2001, respectively. His Ph.D. research work was in vegetation studies at frequencies from 1 to 62.4 GHz. He is currently Head of the Antennas & Propagation (A&P-Lr) Research Group, Instituto de Telecomunicações, Leiria, and a Coordinator Professor in mobile communications with the School of Technology and Management (ESTG), Polytechnic Institute of Leiria (IPLeiria), Portugal. His research interests include the studies of radiowave propagation through vegetation media, radio channel sounding, and modeling and frequency selective surfaces, for applications at microwave and millimeter-wave frequencies. He has authored or coauthored more than 150 papers in conferences and international journals and four contributions to ITU-R Study Group, which formed the basis of the ITU-R P.833-5 (2005) recommendation. He is a Senior Member of the IEEE and a Fellow Member of the IET. He has been the Chair of the IEEE Portugal Joint Chapter on Antennas & Propagation—Electron Devices—Microwave Theory & Techniques, since 2016 and a Regional Delegate of the European Association for Antennas and Propagation (EurAAP) for Andorra, Portugal, and Spain, since 2017. He is the Program Chair of the WINSYS International Conference, from 2006 to 2012. He is an Associate Editor of the IEEE TRANSACTIONS ON ANTENNAS AND PROPAGATION and the *IET on Microwaves, Antennas and Propagation*, a member of the Editorial Board of the *International Journal of Communication Systems* (IJCS) (New York, Wiley), and an Appointed Officer for Awards and Recognitions of the IEEE Portugal Section, in 2014.